Kinetics, Thermodynamics, and Effect of BPh₃ on Competitive C−C and C−H Bond Activation Reactions in the Interconversion of Allyl Cyanide by [Ni(dippe)]

Nicole M. Brunkan,[†] Donna M. Brestensky,[‡] and William D. Jones*,[†]

Contribution from the Department of Chemistry, University of Rochester, Rochester, New York 14627, and Chemistry Department, Box BG, St. Bonaventure University, St. Bonaventure, New York 14778

Received July 1, 2003; E-mail: jones@chem.rochester.edu

Abstract: Reaction of [(dippe)Ni(μ-H)]₂ with allyl cyanide at low temperature quantitatively generates the η^2-olefin complex (dippe)Ni(CH₂=CHCH₂CN) (**1**). At ambient temperature or above, the olefin complex is converted to a mixture of C−CN cleavage product (dippe)Ni(η^3-allyl)(CN) (**3**) and the olefin-isomerization products (dippe)Ni(η^2-crotonitrile) (*cis*- and *trans*-**2**), which form via C−H activation. The latter are the exclusive products at longer reaction times, indicating that C−CN cleavage is reversible and the crotononitrile complexes **2** are more thermodynamically stable than η^3-allyl species **3**. The kinetics of this reaction have been followed as a function of temperature, and rate constants have been extracted by modeling of the reaction. The rate constants for C−CN bond formation (the reverse of C−CN cleavage) show a stronger temperature dependence than those for C−CN and C−H activation, making the observed distribution of C−H versus C−CN cleavage products strongly temperature-dependent. The activation parameters for the C−CN formation step are also quite distinct from those of the C−CN and C−H cleavage steps (larger $\Delta H^\ddagger$ and positive $\Delta S^\ddagger$). Addition of the Lewis acid BPh₃ to **1** at low temperature yields exclusively the C−CN activation product (dippe)Ni(η^3-allyl)(CNBPh₃) (**4**). Independently prepared (dippe)Ni(crotononitrile-BPh₃) (*cis*- and *trans*-**7**) does not interconvert with **4**, indicating that **4** is the kinetic product of the BPh₃-mediated reaction. On standing in solution at ambient temperature, **4** decomposes slowly to complex **5**, with structure [(dippe)Ni(η^3-allyl)(N≡C−BPh₃), while addition of a second equivalent of BPh₃ immediately produces [(dippe)-Ni(η^3-allyl)]⁺[Ph₃BC≡NBPh₃]⁻ (**6**). Comparison of the barriers to $\pi-\sigma$ allyl interconversion (determined via dynamic ¹H NMR spectroscopy) for all of the η^3-allyl complexes reveals that axial cyanide ligands facilitate $\pi-\sigma$ interconversion by moving into the P₂Ni square plane when the allyl group is σ-bound.

Introduction

Reactions that make and break carbon−carbon σ bonds are essential to organic synthesis on both the laboratory and the industrial scale. Although often accomplished by organic reagents, these transformations may also be effected by organometallic reagents that cleave C−C σ bonds via insertion of the transition metal center into the bond.[1] The most widely recognized industrial process involving C−C bond activation by a transition metal complex is DuPont's synthesis of adiponitrile (ADN) via hydrocyanation of butadiene, which is catalyzed by triaryl phosphite−Ni(0) complexes.[2]

The commercial ADN process begins with Ni-catalyzed addition of HCN to butadiene, forming the desired anti-Markovnikov product 3-pentenenitrile (3PN) and the Mark-ovnikov byproduct 2-methyl-3-butenenitrile (2M3BN) in a 2:1 ratio. The unwanted 2M3BN is then isomerized, using the same Ni catalyst, to 3PN through a C−CN bond activation route involving a relatively stable, spectroscopically observable Ni(II) π-allyl cyanide intermediate (eq 1).[2] Further isomerization of 3PN to the terminal cyanoolefin 4-pentenenitrile in the presence of a Ni(0) catalyst and Lewis acid cocatalyst, followed by a second anti-Markovnikov addition of HCN to the olefin, yields ADN. Although the mechanisms of the ADN process and related Ni-catalyzed hydrocyanation reactions have been investigated extensively by DuPont[3] and others,[4] isolation and full characterization of the organometallic Ni complexes involved in the C−C bond activation (2M3BN−3PN isomerization) step have not been reported in the literature.

† University of Rochester.

‡ St. Bonaventure University.

(1) For reviews of C−C bond activation by organometallic complexes, see: (a) Murakami, M.; Ito, Y. In *Topics in Organometallic Chemistry*; Murai, S., Ed.; Springer-Verlag: New York, 1999; pp 97−129. (b) Rybtchinski, B.; Milstein, M. *Angew. Chem., Int. Ed.* **1999**, *38*, 870−883. (c) Perthuisot, C.; Edelbach, B. L.; Zubris, D. L.; Simhai, N.; Iverson, C. N.; Müller, C.; Satoh, T.; Jones, W. D. *J. Mol. Catal. A* **2002**, *189*, 157−168.

(2) McKinney, R. J. In *Homogeneous Catalysis*; Parshall, G. W., Ed.; Wiley: New York, 1992; pp 42−50.

(3) (a) Tolman, C. A.; McKinney, R. J.; Seidel, W. C.; Druliner, J. D.; Stevens, W. R. *Adv. Catal.* **1985**, *33*, 1−47. (b) Seidel, W. C.; Tolman, C. A. *Ann. N.Y. Acad. Sci.* **1983**, *201*−221.

(4) (a) Goertz, W.; Kamer, P. C. J.; van Leeuwen, P. W. N. M.; Vogt, D. *Chem.-Eur. J.* **2001**, *7*, 1514−1618. (b) Goertz, W.; Keim, W.; Vogt, D.; Englert, U.; Boele, M. D. K.; van der Veen, L. A.; Kamer, P. C. J.; van Leeuwen, P. W. N. M. *J. Chem. Soc., Dalton Trans.* **1998**, 2981−2988. (c) Bäckvall, J. E.; Andell, O. S. *Organometallics* **1986**, *5*, 2350−2355. (d) Taylor, B. W.; Swift, H. E. *J. Catal.* **1972**, *26*, 254−260. (e) Keim, W.; Behr, A.; Lühr, H.-O.; Weisser, J. *J. Catal.* **1982**, *78*, 209−216. (f) Campi, E. M.; Elmes, P. S.; Jackson, W. R.; Lovel, C. G.; Probert, M. K. S. *Aust. J. Chem.* **1987**, *40*, 1053−1061.

$$(1)$$
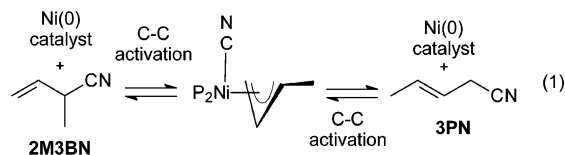
C−CN bond cleavage of nitrile substrates other than 2M3BN by organometallic species has been studied,[5] as has the reverse reaction of C−CN reductive elimination from transition metal complexes.[6] We recently reported reversible C−CN bond activation of substituted benzonitriles, cyanopyridines, and cyanoquinones by the electron-rich (dippe)Ni(0) fragment (dippe = 1,2-bis(diisopropylphosphino)ethane), which is generated from the hydride dimer [(dippe)Ni(μ-H)]$_2$ upon loss of H$_2$.[7] η^2-Coordination of the ArCN cyano group to Ni(0) yields isolable, fully characterized (dippe)Ni(η^2-N≡CAr) complexes, which undergo reversible C−CN oxidative addition reactions to give isolable Ni(II) (dippe)Ni(Ar)(CN) products.

Because of their relevance to the ADN process, reactions of allylic cyanide substrates with [(dippe)Ni(μ-H)]$_2$ were then examined. Herein, we describe the kinetically competitive C−H and C−CN bond activation reactions that allyl cyanide, the simplest of this substrate class, undergoes upon coordination to (dippe)Ni(0) (work with the more complicated substrate 2M3BN is ongoing). Reaction of allyl cyanide with (dippe)Ni-(0) in the presence of the Lewis acid BPh$_3$ was also examined, as literature reports indicate that Lewis acids facilitate C−CN cleavage in the DuPont phosphite−Ni system.[3,8] The availability of structural and spectroscopic information for nearly all of the organometallic species involved in the interconversion of allyl cyanide by (dippe)Ni(0), in both the presence and the absence of the Lewis acid BPh$_3$, provides a unique opportunity to directly compare C−H and C−C activation processes, and the effect of Lewis acids on them, in a single well-defined system. Kinetic data for the interconversion of these species at different temperatures also provide insight into the mechanisms of the fundamentally important and industrially relevant C−H cleavage, C−CN cleavage, and C−CN bond formation reactions observed.

Results and Discussion

Reaction of [(dippe)Ni(μ-H)]$_2$ with Allyl Cyanide at −78 °C. The hydride dimer [(dippe)Ni(μ-H)]$_2$ acts as a source of the highly reactive fragment (dippe)Ni(0), as it readily loses H$_2$ upon exposure to a variety of neutral, often weakly coordinating ligands and produces (dippe)Ni(0)−ligand complexes.[9] Upon mixing allyl cyanide (1 equiv per Ni center) with

a very dark red THF-d_8 solution of the hydride dimer at −78 °C, evolution of H$_2$ gas and a color change to yellow-brown were observed. ^{31}P{^{1}H} and ^{1}H NMR spectra of the reaction mixture at −30 °C showed quantitative conversion of the starting material to the Ni(0) η^2-olefin complex (dippe)Ni(allyl cyanide) (**1**), producing a pair of doublets at 72.1 and 66.9 ppm with $^2J_{P-P}$ = 60 Hz in the ^{31}P NMR spectrum (eq 2).

$$(2)$$
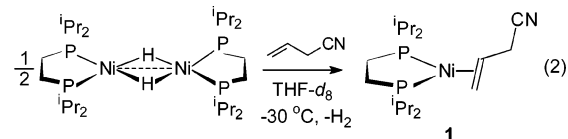
Characterization of the η^2-Olefin Complex 1. While product **1** could not be isolated because it isomerized rapidly at temperatures above −30 °C (vide infra), it was identified as an η^2-olefin complex on the basis of its NMR data. The ^{31}P NMR spectrum of **1** is similar to that of the previously reported (dippe)Ni(0) η^2-olefin complex of 3-cyanoquinoline (**A**; δ 65.9, d; δ 60.9, d, $^2J_{P-P}$ = 54 Hz), which was characterized by NMR spectroscopy and X-ray crystallography.[7b] The small P−P coupling constant is not consistent with η^2-C≡N coordination, which in (dippe)Ni(ArCN) complexes produces $^2J_{P-P}$ between 63 Hz (electron-deficient ArCN) and 72 Hz (electron-rich ArCN).[7b] Because the allyl group of allyl cyanide is more electron-donating than even the most electron-rich aryl group of the nitriles previously investigated, a P−P coupling constant greater than 72 Hz is expected for a Ni(0) η^2-CN allyl cyanide complex, in contrast to the observed data for **1**.[10] The small difference in chemical shift between the ^{31}P doublets of **1** ($\Delta\delta$ 5.2 ppm) also resembles **A** rather than the η^2-CN-bonded (dippe)Ni(ArCN) complexes ($\Delta\delta \approx$ 12 ppm).[7b]
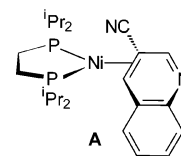
The ^{1}H NMR spectrum of **1** is consistent with η^2-C═C coordination of allyl cyanide to Ni. Although one of the multiplets for the olefin protons could not be distinguished from those of the four magnetically inequivalent methine protons of the dippe ligand due to extensive overlap, all resonances in the complex appear upfield of 2.77 ppm,[11] whereas the olefin protons of free allyl cyanide resonate between 5.2 and 5.8 ppm. Eight distinct resonances (each a doublet of doublets due to coupling to P and the ^{i}Pr methine proton) were observed for the eight methyl groups of the dippe ligand, indicating that rotation around the Ni−olefin bond does not occur at −30 °C. In the −30 °C ^{13}C{^{1}H} NMR spectrum of **1**, the olefin carbons of allyl cyanide are shifted far upfield from their positions in the free ligand (128.4 and 119.1 ppm) to 38.5 and 33.5 ppm, consistent with η^2-C═C coordination to Ni(0). Both appear as doublets of doublets due to coupling with the *trans* and *cis* phosphorus atoms of **1** (Table 1). The methylene carbon of allyl

(5) (a) Miller, J. A. *Tetrahedron Lett.* **2001**, *42*, 6991. (b) Taw, F. L.; White, P. S.; Bergman, R. G.; Brookhart, M. *J. Am. Chem. Soc.* **2002**, *124*, 4192−4193. (c) Churchill, D.; Shin, J. H.; Hascall, T.; Hahn, J. M.; Bridgewater, B. M.; Parkin, G. *Organometallics* **1999**, *18*, 2403.

(6) (a) Yamamoto, T.; Yamaguchi, I.; Abla, M. *J. Organomet. Chem.* **2003**, *671*, 179−182. (b) Huang, J.; Haar, C. M.; Nolan, S. P.; Marcone, J. E.; Moloy, K. G. *Organometallics* **1999**, *18*, 297−299. (c) Marcone, J. E.; Moloy, K. G. *J. Am. Chem. Soc.* **1998**, *120*, 8527−8528. (d) Favero, G.; Gaddi, M.; Morvillo, A.; Turco, A. *J. Organomet. Chem.* **1978**, *149*, 395−400.

(7) (a) Garcia, J. J.; Jones, W. D. *Organometallics* **2000**, *19*, 5544−5545. (b) Garcia, J. J.; Brunkan, N. M.; Jones, W. D. *J. Am. Chem. Soc.* **2002**, *124*, 9547−9555.

(8) Tolman, C. A.; Seidel, W. C.; Druliner, J. D.; Domaille, P. J. *Organometallics* **1984**, *3*, 33−38.

(9) For examples, see: (a) Edelbach, B. L.; Vicic, D. A.; Lachicotte, R. J.; Jones, W. D. *Organometallics* **1998**, *17*, 4784. (b) Edelbach, B. L.; Vicic, D. A.; Lachicotte, R. J.; Jones, W. D. *Organometallics* **1999**, *18*, 4040. (c) Müller, C.; Iverson, C. N.; Lachicotte, R. J.; Jones, W. D. *J. Am. Chem. Soc.* **2001**, *123*, 9718−9719.

(10) We have since observed several η^2-C≡N complexes of allylic nitriles by ^{31}P and ^{1}H NMR spectroscopy at low temperature in THF-d_8 solution; all exhibit P−P coupling constants greater than 72 Hz. For example, $^2J_{P-P}$ = 74 Hz for (dippe)Ni(η^2-CN-3-pentenenitrile).

(11) See Supporting Information for the ^{1}H NMR spectrum.

Table 1. Selected NMR and IR Data for **2**−**7**

	^{31}P{^{1}H} NMR			^{1}H NMR				^{13}C{^{1}H} NMR				IR
	m	δ (ppm)	$^2J_{P-P}$ (Hz)	m^c	δ (ppm)	J_{H-X} (Hz)	ass.	m	δ (ppm)	J_{C-P} (Hz)	ass.	ν_{CN} (cm^{-1})
1	d	72.1	60	m	<2.77		all H	d	121.5	6.7	*CN*	
	d	66.9						dd	38.5	25.6, 2.2	=*C*H$_2$	
								dd	33.5	20.9^a	=*C*(H)CH$_2$CN	
								dd	26.4	17.0, 4.0	*C*H$_2$CN	
trans-**2**	d	70.8	53	m	<2.51		all H	t	125.5	4.6	^{13}*C*N	2181
	d	67.8		td	1.25	7.2, 1.6	CH$_3$	d	43.1	27.3	=*C*(H)CH$_3$	
						1.6		d	26.4	3.3	=*C*(H)CN	
cis-**2**	d	70.2	54	m	<2.42		all H	dd	124.6	5.6, 2.5	^{13}*C*N	2181
	d	67.0		td	1.39	7.4, 1.6	CH$_3$	d	40.1	27.2	=*C*(H)CH$_3$	
								d	26.2	3.5	=*C*(H)CN	
3	s	80.8		5t	4.73	9.0, 2.4	H$_a$	t	154.8	10.3	^{13}*C*N	2096
				d	2.97	9.0	H$_{b/c}$	t	89.7	1.6	allyl *C*H	
								t	53.7	9.0	allyl *C*H$_2$	
4	s	84.2		5t	4.89	9.2, 2.4	H$_a$	t	156.4	12.1	^{13}*C*NBPh$_3$	2150
				d	3.15	7.2	H$_{b/c}$	t	93.1	a	allyl *C*H	
								t	55.5	8.2	allyl *C*H$_2$	
5	s	79.5		m	5.00		H$_a$	br s	148.2		^{13}*C*N	2182
					4.22	3	H$_b$	s	111.5		allyl *C*H	
					2.54	13, 3	H$_c$	d	62.79	14.0	allyl *C*H$_2$	
6	s	83.0		m	5.00	(b)	H$_a$	br	139.3		B^{13}*C*NB	2245
				d	4.40	7.2	H$_b$	s	117.1		allyl *C*H	
				d	2.43	14.4	H$_c$	dd	64.7	12.4, 2.0	allyl *C*H$_2$	
trans-**7**	d	71.8	44	m	<2.71		=CH		a		*C*NBPh$_3$	2244
	d	69.1		td	1.39	5.6, 2.4	CH$_3$	d	41.4	30.4	=*C*(H)CH$_3$	
								d	26.6	3.8	=*C*(H)CNB	
cis-**7**	d	71.8	44	m	<2.55		=CH	s	122.9		*C*NBPh$_3$	2244
	d	68.7		td	1.39	5.6	CH$_3$	d	39.1	29.2	=*C*(H)CH$_3$	
								d	26.4	3.6	=*C*(H)CNB	

^{a} Too small to measure. ^{b} Seven-line multiplet at room temperature; quintet at higher temperatures. ^{c} For **3** and **4**, "5t" = quintet of triplets.

Scheme 1

cyanide also gives a doublet of doublets at 26.4 ppm, while the cyano carbon is a doublet (J_{C-P} = 6.7 Hz) at 121.5 ppm, slightly downfield of the CN of free allyl cyanide (118.0 ppm). Similar ^{13}C NMR shifts have previously been noted on coordination of acrylonitrile to P$_2$Ni or P$_2$Pt complexes (vide infra).[12]

Competitive C−H and C−C Bond Activation in 1. When the THF-d_8 solution of **1** was warmed to 20 °C or above, several new species rapidly grew in at the expense of **1**. Two sets of doublets, the major resonances observed by ^{31}P NMR spectroscopy, appeared at 70.8 and 67.8 ppm with $^2J_{P-P}$ = 53 Hz, and at 70.2 and 67.0 ppm with $^2J_{P-P}$ = 54 Hz, consistent with the formation of two new Ni(0) η^2-olefin complexes. Independent synthesis and full characterization of these species (vide infra) revealed that they are η^2-olefin complexes of *trans*- and *cis*-crotononitrile (*trans*-**2** and *cis*-**2**), formed from **1** by isomerization of the double bond of allyl cyanide into the position conjugated with the cyano group (Scheme 1). Crotononitrile is thermodynamically more stable than allyl cyanide by 4−5 kcal mol^{-1} and coordinates more strongly to Ni(0) because the electron-withdrawing CN substituent is bound directly to the olefin, providing a driving force for this transformation.[13] Conversion of **1** to **2** is proposed to occur via the C−H bond activation mechanism shown in Scheme 1. This pathway probably involves a reactive Ni(II) hydride intermediate, although no hydrides were observed by ^{1}H NMR spectroscopy during the reaction, even at −80 °C. Slightly more *trans*- than
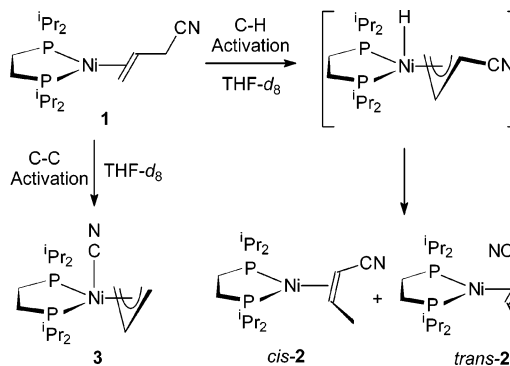
cis-**2** is formed during the reaction, and the ratio of *trans*-**2**:*cis*-**2** remains constant throughout (1.35:1 ratio at 40 °C; Figure 1).

A third species (**3**) was also observed in the ^{31}P NMR spectrum of the reaction as a singlet at 80.8 ppm. This resonance grew in rapidly, reached a maximum that varied with temperature, and then decreased slowly until it disappeared, leaving **2** as the sole product of the reaction. Figure 1 shows the distribution of species over time (measured via integration of a series of ^{31}P NMR spectra) for a typical reaction at 40 °C.[14] A ^{1}H NMR spectrum of the reaction, taken when **3** was at a maximum, included a quintet of triplets at 4.73 ppm (J_{H-H} = 9.0 Hz, J_{H-P} = 2.4 Hz, 1H) and a doublet at 2.97 ppm (J_{H-H} = 9.0 Hz, 4H) that were assigned to **3**. These resonances are typical of a Ni(II) π-allyl complex whose allyl *syn* and *anti*

(12) (a) Tolman, C. A.; English, A. D.; Manzer, L. E. *Inorg. Chem.* **1975**, *14*, 2353−2356. (b) Pellizer, G.; Lenarda, M.; Ganzerla, R.; Graziani, M. *Gazz. Chim. Ital.* **1986**, *116*, 155−161.

(13) Afeefy, H. Y.; Liebman, J. F.; Stein, S. E. Neutral Thermochemical Data. In *NIST Chemistry WebBook, NIST Standard Reference Database Number 69*; Linstrom, P. J., Mallard, W. G., Eds.; National Institute of Standards and Technology: Gaithersburg, MD 20899 (http://webbook.nist.gov), March 2003.

(14) A similar distribution of species plot (obtained by IR spectroscopy) for the [P(OEt)$_3$]$_4$Ni-catalyzed addition of HCN to butadiene at 35 °C shows that the intermediate P$_2$Ni(π-1-methallyl)CN behaves much like **3**, except that it grows in more slowly (reaching a maximum after 5 h of reaction time) and disappears more rapidly than **3**.[3]
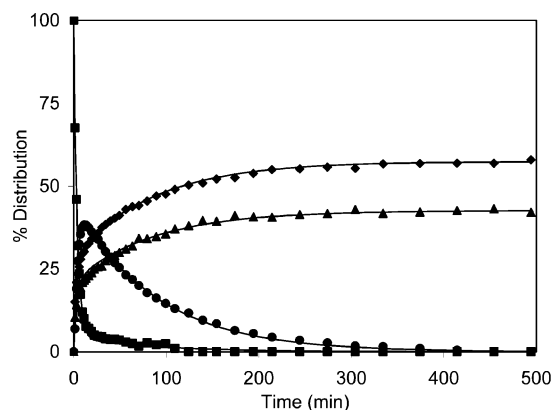
Figure 1. Distribution of species **1** (■), *trans*-**2** (◆), *cis*-**2** (▲), and **3** (●) for the reaction shown in Scheme 1 at 40 °C.

protons are equilibrated on the NMR time scale by rapid $\pi-\sigma$ interconversion of the allyl ligand.[15] Thus, **3** was identified as the Ni(II) C–CN bond activation product (dippe)Ni(π-allyl)-CN (Scheme 1). Independent synthesis and full characterization of (dippe)Ni(π-allyl)CN (reported elsewhere,[16] although some data are reproduced in Tables 1 and 2) yielded spectroscopic data identical to that observed for **3** during the rearrangement of **1**, unambiguously confirming its identity. X-ray diffraction revealed that **3** has a square pyramidal structure with the cyano ligand in the apical position, and dynamic ^{1}H NMR experiments demonstrated that conversion of the allyl ligand from π- to σ-bound ($\Delta G^{\ddagger} = 9.3$ kcal mol^{-1} at −68 °C) allows the cyano ligand to move into the Ni(II) square plane, interconverting "CN-up" and "CN-down" conformers of **3** and rendering all four [i]Pr groups of the dippe ligand equivalent (see Supporting Information).[16]

Although red crystals of **3** are indefinitely stable under inert atmosphere, a solution of **3** in THF-d_8 was completely converted to *trans*- and *cis*-**2** (1.13:1 ratio) upon standing at room temperature for 5 d, just as **3** is converted to **2** during rearrangement of **1** (Figure 1). This transformation requires that the C–C bond cleavage reaction is reversible and that **2** is more thermodynamically stable than **3** (Scheme 1).

Characterization of the Crotononitrile Complexes 2. The ^{31}P NMR spectra of *trans*- and *cis*-**2** (Table 1) are consistent with their formulation as crotononitrile complexes. The decrease in $^2J_{P-P}$ for these species as compared to **1**, which indicates stronger binding of the olefin to Ni, is particularly convincing evidence that the C=C bond in **2** is conjugated with the cyano group (as in the η^2-C=C 3-cyanoquinoline complex **A**, which has almost exactly the same P–P coupling constant as **2**). The room-temperature ^{1}H NMR spectrum obtained for the final products of the reaction, a mixture of *trans*- and *cis*-**2**, also supports this assignment. The protons on the Ni(0)-coordinated double bonds could not be distinguished from the methine protons of dippe, but all resonances of the complexes appear upfield of 2.51 ppm,[11] while the olefin resonances for free crotononitrile appear between 5.4 and 6.8 ppm. Similarly large upfield shifts (1.75–4.01 ppm) for the protons of acrylonitrile have previously been reported upon coordination to a bis-

(phosphite) L$_2$Ni(0) fragment [L = P(O-*o*-tol)$_3$].[12a,17] The methyl groups of *trans*- and *cis*-crotononitrile were assigned as triplets of doublets (due to coupling with P and =C(*H*)CH$_3$) at 1.25 and 1.39 ppm, respectively. As in **1**, eight distinct doublets of doublets were observed for the eight methyl groups of the dippe ligand in each complex, indicating that the crotononitrile ligands do not rotate rapidly at room temperature.

A yellow crystal suitable for X-ray diffraction yielded the structure of the major isomer *trans*-**2** (Figure 2). Selected bond lengths and angles for the complex are given in Table 2. The olefin carbons C2 and C3 lie approximately in the P$_2$Ni square plane and are nearly equidistant from Ni at 1.959(2) and 1.949(2) Å, respectively. The olefin in **2** binds much more symmetrically to Ni(0) than acrylonitrile (ACN) does in the complex [P(O-*o*-tol)$_3$]$_2$Ni(ACN), for which Ni–C distances that differ by 0.10 Å were measured (shorter bond to the CN-substituted carbon; 2.016(10) vs 1.911(12) Å).[18] The olefin bond length C2–C3 in **2** is comparable to that of the acrylonitrile complex (1.441(4) vs 1.46(2) Å), while the C≡N bond distance is slightly shorter (1.151(4) vs 1.20(2) Å).

Reaction of [(dippe)Ni(μ-H)]$_2$ with a stoichiometric amount of a commercially available 1:2 mixture of *trans*- and *cis*-crotononitrile afforded *trans*- and *cis*-**2** in a 1:2 ratio, with NMR spectra identical to those of the species formed during rearrangement of **1** (eq 3). Observation of an isomer ratio (which does not change upon heating at 55 °C for several days) different from the one obtained by isomerization of **1** indicates that *trans*-**2** and *cis*-**2** do not interconvert under the reaction conditions. In other words, the C–H bond activation pathway in Scheme 1 is effectively irreversible, unlike the C–C bond activation pathway. Thus, the ∼1.35:1 *trans*-**2**:*cis*-**2** ratio produced by allyl cyanide isomerization reflects a small kinetic preference for activation of one of the diastereotopic –C*H*$_2$CN protons of allyl cyanide over the other one, producing more *trans*- than *cis*-crotononitrile. The complexes **2** were also prepared in a 1:2 ratio on a larger scale by reaction of (dippe)-Ni(COD) with crotononitrile, and nearly pure (97%) *cis*-**2** was isolated by fractional recrystallization of the 1:2 product mixture.

$$(3)$$
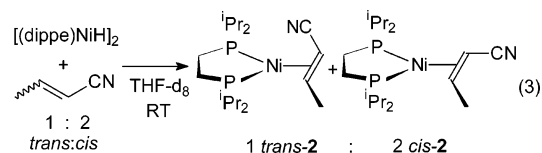
IR spectra of **2** (pure *cis* or a *cis*–*trans* mixture) in THF contain a single C≡N stretching band at 2181 cm^{-1}, 40 cm^{-1} lower than $\nu_{CN} = 2221$ cm^{-1} for free crotononitrile. This decrease in ν_{CN} reflects the weakening of the C≡N bond by electron donation from the d^{10} Ni(0) center into the C≡N π^* orbital. The decrease in ν_{CN} for crotononitrile upon binding to the (dippe)Ni(0) fragment is larger than the 32–33 cm^{-1} change observed on coordination of acrylonitrile to (Ph$_3$P)$_2$Ni(0) or [P(O-*o*-tol)$_3$]$_2$Ni(0) ($\nu_{CN} = 2195$ and 2194 cm^{-1}, respectively)[17] and the 26–28 cm^{-1} decrease observed on binding of *trans*- or *cis*-crotononitrile to (*t*BuNC)$_2$Ni(0) ($\nu_{CN} = 2195$ and 2193 cm^{-1}),[19] suggesting that (dippe)Ni(0) is more electron-donating

(15) Wilke, G.; Bogdanović, B.; Hardt, P.; Heimbach, P.; Keim, W.; Kröner, M.; Oberkirch, W.; Tanaka, K.; Steinrücke, E.; Walter, D.; Zimmerman, H. *Angew. Chem., Int. Ed. Engl.* **1966**, *5*, 151–266.
(16) Brunkan, N. M.; Jones, W. D. *J. Organomet. Chem.* **2003**, *683*, 77–82.

(17) Tolman, C. A.; Seidel, W. C. *J. Am. Chem. Soc.* **1974**, *96*, 2774–2780.
(18) Guggenberger, L. J. *Inorg. Chem.* **1973**, *12*, 499–508.
(19) Ittel, S. D. *Inorg. Chem.* **1977**, *16*, 2589–2597.

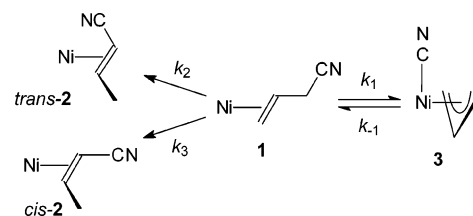***Table 2.*** Selected Bond Distances (Å) and Angles (deg) for **2**−**7**

	trans-**2**	cis-**7**	**3**[a]	**4**	**6**
N−B1		1.612(5)		1.592(2)	1.645(8),[b] 1.677(9)[c]
C1−B2					1.549(10), 1.548(10)
C1≡N	1.151(4)	1.151(4)	1.146(4), 1.149(4)	1.1517(19)	1.167(9), 1.138(9)
C2=C3	1.441(4)	1.442(5)	1.399(4), 1.401(4)	1.399(2)	1.390(4)
C3=C4			1.402(4), 1.392(4)	1.391(2)	1.366(4)
Ni−C1			1.994(3), 1.983(3)	1.9835(15)	
Ni−C2	1.959(2)	1.961(4)	2.084(3), 2.078(3)	2.0992(16)	2.023(2)
Ni−C3	1.949(2)	1.933(4)	1.997(3), 1.990(3)	2.0080(16)	2.001(2)
Ni−C4			2.090(3), 2.098(3)	2.0823(16)	2.025(3)
Ni−P1	2.1434(7)	2.1465(11)	2.1916(8), 2.1847(8)	2.2002(4)	2.1564(7)
Ni−P2	2.1674(7)	2.1750(10)	2.1894(9), 2.1899(8)	2.1899(4)	2.1608(7)
P1−Ni−P2	91.64(2)	93.33(4)	88.72(3), 89.06(3)	89.103(16)	91.00(3)
C2−C3−C4			117.2(3), 117.6(3)	118.78(16)	120.6(3)
C2−Ni−C3	43.28(11)	43.46(14)			
Ni−C1−C2	111.18(18)	111.6(3)			
C2−C1≡N	179.4(3)	178.7(4)			
C1≡N−B1		174.4(3)		175.12(15)	176.6(11), 175.3(12)
N≡C1−B2					177.7(13), 175.6(14)
Ni−C1≡N			177.7(3), 176.5(3)	171.05(14)	

[a] Two molecules in the unit cell. *[b]* B2−C1−N1−B1 isomer. *[c]* B1−C1−N1−B2 isomer.
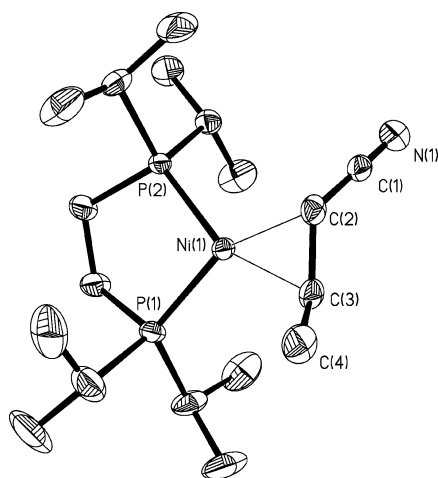

Figure 2. ORTEP drawing of *trans*-**2** showing 30% probability ellipsoids.

and a better π-back-bonder than the Ni(0) centers supported by aryl-phosphine, phosphite, or isocyanide ligands.

A clean 1.13:1 mixture of *trans*- and *cis*-¹³CN-labeled **2** was obtained by allowing a THF-*d*₈ solution of ¹³CN-labeled **3**[16] to stand at room temperature for 112 h (eq 4). The −20 °C ¹³C{¹H} NMR spectrum of this mixture contained a triplet ($J_{P–C}$ = 4.6 Hz) for the labeled ¹³*C*N of *trans*-**2** at 125.5 ppm and a doublet of doublets (*trans*- and *cis*-P coupling of 5.6 and 2.5 Hz, respectively) for the labeled ¹³*C*N of *cis*-**2** at 124.6 ppm (Table 1).[20] These chemical shifts are similar to δ_{CN} of **1** and almost identical to the CN shift of 125.5 observed for Pt(0)-coordinated acrylonitrile in the complex (Ph₃P)₂Pt(ACN).[12b] Like the olefin protons in the ¹H NMR spectra of **2**, the olefin carbons of crotononitrile are also shifted far upfield upon coordination to (dippe)Ni(0). The =*C*(H)CH₃ carbons of *trans*- and *cis*-**2** give doublets at 43.1 and 40.1 ppm, respectively, in good agreement with the 42.7 ppm shift observed for =*C*H₂ in [P(O-*o*-tol)₃]₂Ni-(ACN).[12a] Doublets at 26.4 and 26.2 ppm were assigned to the

(20) Resonances for *trans*- and *cis*-**2** were assigned by comparison of the ¹³C{¹H} NMR spectrum of the mixture to the ¹³C{¹H} NMR spectrum of unlabeled, 97% *cis*-**2**.

Scheme 2

=*C*(H)¹³CN carbons of *trans*- and *cis*-**2**, in accordance with the 25.9 ppm shift of =*C*(H)CN in the acrylonitrile complex.[21]
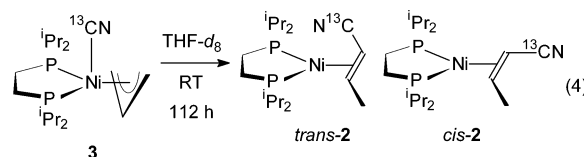
Kinetic Distribution of C−H versus C−C Bond Activation Products and Their Variation with Temperature. Although C−C bond activation in **1** is thermodynamically less favorable than C−H bond activation, the C−C and C−H bond cleavage reactions in Scheme 1 are kinetically competitive (Figure 1). The kinetic distribution of C−H activation products **2** versus C−C activation product **3**, defined as the ratio (sum of rate constants for formation of **2**)/(rate constant for formation of **3**), was determined at five different temperatures between 20 and 50 °C as described below. Variation of the rate constants with temperature yielded the activation parameters $\Delta H^{\ddagger}$ and $\Delta S^{\ddagger}$ for C−H and C−C bond activation of **1**, as well as C−C reductive elimination from **3**.

Values for the rate constants k_1 (**1** → **3**), k_{-1} (**3** → **1**), k_2 (**1** → *trans*-**2**), and k_3 (**1** → *cis*-**2**), defined in Scheme 2, were determined at 40 °C by simulation of the concentration versus time data shown in Figure 1. The program KINSIM provided a rough fit to the data, and then a least-squares fit was calculated

(21) Note that, in addition to the small *cis* C−P coupling constant observed for these resonances, 20−30 Hz coupling to the *trans*-P is also expected, suggesting that the observed doublets each represent one-half of a set of doublets of doublets, whose other halves are obscured by the THF-*d*₈ solvent resonance at 25.4 ppm.
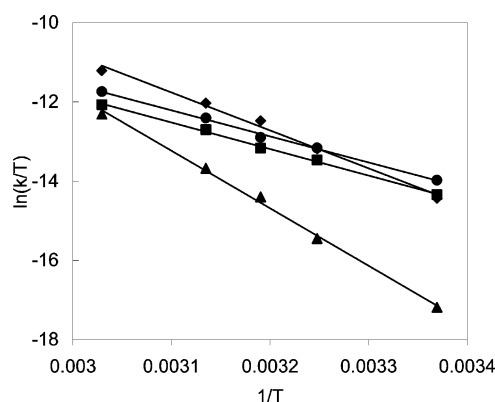
Table 3. Rate Constants for C−H and C−C Activation of **1** at Various Temperatures[a]

temp (°C)	$k_1 \times 10^3$ (min⁻¹)	$k_{-1} \times 10^3$ (min⁻¹)	$k_2 \times 10^3$ (min⁻¹)	$k_3 \times 10^3$ (min⁻¹)	k_2/k_3	[trans-**2**]/ [cis-**2**]	$(k_2 + k_3)/ k_1$
20	9.6(1.2)	0.6(0.2)	15.2(1.3)	10.5(1.0)	1.45	1.48	2.67
30	34.7(2.2)	3.6(0.5)	35.4(1.8)	26.1(1.4)	1.36	1.38	1.77
35	71.5(2.6)	10.5(0.8)	47.0(1.4)	35.8(1.2)	1.31	1.33	1.16
40	113.4(3.5)	22.0(1.3)	78.2(1.9)	58.0(1.5)	1.35	1.37	1.20
50	268(13)	89.1(6.4)	157.5(4.8)	112.9(3.6)	1.40	1.40	1.01

[a] Values in parentheses represent 2σ uncertainty (95% confidence limit).

using the program FITSIM.[22] This least-squares fit is represented by the lines drawn in Figure 1 (points represent experimental data), and the values k_1-k_3 are listed in Table 3. Distribution of species plots such as the one in Figure 1 were also created for reactions at 20, 30, 35, and 50 °C[23] and were fit in the same manner to provide the rest of the rate constants in Table 3. The relative rates of formation of *trans*- versus *cis*-**2** (k_2/k_3; Table 3, column 6) were consistent with the final ratio of *trans*- to *cis*-**2** observed at each temperature (Table 3, column 7), providing a good check of the validity of the calculated rate constants. The kinetic distributions of C−H activation products **2** versus C−C activation product **3** were also calculated from $(k_2 + k_3)/k_1$ at each temperature (Table 3, column 8). Over the temperature range investigated, C−C activation becomes increasingly kinetically competitive with C−H activation as the reaction temperature is raised, until at 50 °C the two processes occur at almost the same rates ($(k_2 + k_3)/k_1 \approx 1$).[24]

C−C cleavage product **3**, however, becomes much less thermodynamically competitive with C−H activation products **2** as the temperature is raised, because the **1** ⇌ **3** equilibrium shifts increasingly to the left at higher temperatures. In other words, kinetic and thermodynamic influences on the concentration of **3** in the reaction solution oppose one another. This situation arises because the rate constants k vary with temperature to different degrees, as is apparent from the Eyring plot in Figure 3. k_{-1} is far more sensitive to changes in temperature than k_1 (making K_{eq} for the **1** ⇌ **3** equilibrium markedly temperature-dependent),[25] which in turn varies more with temperature than the C−H activation constants k_2 and k_3. Thus, at room temperature, C−C bond activation occurs more slowly than C−H bond cleavage, producing less C−C cleavage product **3** than at elevated temperatures (kinetic effect); yet, relatively high concentrations of **3** remain in solution for days because

Figure 3. Eyring plot for rate constants k_1 (◆), k_2 (●), k_3 (■), and k_{-1} (▲).

Table 4. Activation Parameters for C−H and C−C Activation of **1**[a]

	$\Delta H^\ddagger$ (kcal/mol)	$\Delta S^\ddagger$ (eu)	$\Delta G^\ddagger$ at 40 °C (kcal/mol)
k_1	18.0(0.3)	−14.8(0.8)	22.71
k_{-1}	27.5(0.5)	11.7(1.6)	23.75
k_2	13.4(0.2)	−29.9(0.6)	22.95
k_3	13.2(0.2)	−31.2(0.7)	23.14

[a] Uncertainties in parentheses are σ values calculated using a weighted nonlinear least-squares analysis.[26]

the complex is more thermodynamically stable at this temperature (k_{-1} is very small). At elevated temperatures, **3** forms much more rapidly and higher concentrations are observed initially (kinetic effect), but the thermodynamic instability of **3** at these temperatures causes it to disappear completely in <3 h at 50 °C.

The activation parameters for C−C bond cleavage (k_1), C−C bond formation (k_{-1}), and C−H bond cleavage (k_2, k_3) of allyl cyanide by (dippe)Ni(0) were calculated from the Eyring plot (Figure 3, Table 4) using a weighted nonlinear least-squares analysis.[26] The enthalpic cost $\Delta H^\ddagger$ of C−H bond cleavage (identical within experimental error for *trans*- and *cis*-**2** reactions) is less than that of C−C cleavage by about 5 kcal mol⁻¹. However, the enthalpic cost $\Delta H^\ddagger$ of C−C bond cleavage is in turn far less than that of C−C bond formation, by nearly 10 kcal mol⁻¹. Apparently, the rate-determining step of the C−C bond-forming process involves significantly more bond-breaking (metal−allyl and metal−cyanide) than the rate-determining step for C−C bond cleavage. The entropy of activation $\Delta S^\ddagger$ for formation of C−H activation products **2** from **1** is negative and unexpectedly large (~ −30 eu), suggesting that degrees of freedom are significantly reduced in the transition state for isomerization of Ni-bound allyl cyanide to Ni-bound crotononitrile. By comparison, $\Delta S^\ddagger$ for C−C cleavage is only one-half as large, but still negative. In contrast to both of these, $\Delta S^\ddagger$ for C−C bond formation is positive, suggesting a less-ordered transition state.

Scheme 3 shows mechanistic paths that account for these differences. From η^2-allylcyanide complex **1**, π-coordination of the nitrile to give an η^4-intermediate would place the allylic C−H bond in just the proper position for C−H activation, directly giving the π-allyl hydride intermediate from this very

(22) KINSIM Version 3.3, 1983, was written by B. A. Barshop, Department of Biological Chemistry, Washington University Medical School, St. Louis, MO 63110. See: Barshop, B. A.; Wrenn, R. F.; Frieden, C. *Anal. Biochem.* **1983**, *130*, 134−145. FITSIM Version 1.63, 1987, was developed by C. T. Zimmerle. See: Zimmerle, C. T.; Patane, K.; Frieden, C. *Biochemistry* **1987**, *26*, 6545−6552. For reviews of kinetic regression analysis methods, see: (a) Mannervick, B. *Methods Enzymol.* **1982**, *63*, 103−139. (b) Motulsky, H. J.; Ransnas, L. A. *FASEB J.* **1987**, *1*, 363−374.

(23) Experiments at temperatures outside this range proved impractical, as reactions above 50 °C became too rapid to monitor by ³¹P NMR spectroscopy and reactions below 20 °C were too slow (>48 h reaction time) to leave in the NMR probe continuously. Also, at low temperatures, only small amounts of **3** were formed (<5% at 0 °C), making accurate integration difficult. Note that slightly poorer fits to the data are obtained at lower temperatures; see Supporting Information.

(24) The trend toward less C−C activation at low temperatures is also supported by qualitative data collected at 0 °C (the maximum amount of **3** observed during the reaction was <5%) and −30 °C (no C−C bond cleavage was observed).

(25) By contrast, raising the temperature from 35 to 50 °C during the [P(OEt)₃]₄Ni-catalyzed addition of HCN to butadiene increases the rates for both formation and decay of intermediate P₂Ni(1-methyl-π-allyl)CN by the same amount (6 times faster).[3a] Note that the intermediate forms via a different route than **3**, however, so its formation rate constant is not expected to be analogous to k_1.

(26) The nonlinear least squares program LSM was used to calculate the activation parameters from the rate constants and their errors. The program is available free of charge from the author, J. A. Mamczur, Institute of Physics, Rzeszow University of Technology, Al. Powstancow Warszawy 6, 35-959 Rzeszow, Poland, http://www.prz.rzeszow.pl/~janand/.

Scheme 3
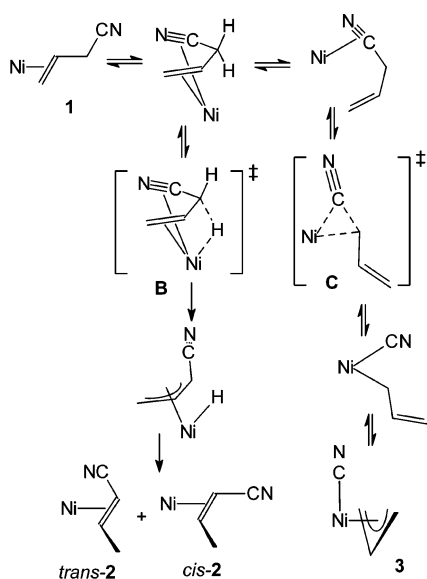
ordered transition state (**B**). Alternatively, release of the olefin portion of the substrate to give an η^2-nitrile complex could then lead to cleavage of the C–C bond to give a square planar Ni(II) σ-allyl cyanide complex that then closes to give π-allyl product **3**. This pathway is a direct analogy to the established mechanism of cleavage of C–CN bonds in aryl nitriles by [(dippe)Ni^0],[7] which occurs from the η^2-CN complex. This transition state (**C**) is also ordered, but less so than the transition state for C–H cleavage (**B**) because there is a freely dangling vinyl group, so a smaller negative $\Delta S^‡$ is expected. By the principle of microscopic reversibility, if this pathway is indeed operative for C–CN cleavage, then the same pathway must be followed for C–CN bond formation. That is, the π-allyl complex **3** must first rearrange to the σ-allyl cyanide complex and then undergo reductive coupling of the C–C bond via **C**. This transition state, with the freely dangling vinyl group, would have less order than the π-allyl complex **3**, and therefore can accommodate the positive $\Delta S^‡$ for the C–CN formation step of the reaction. The large positive $\Delta H^‡$ of this step is also consistent with the π-allyl to σ-allyl rearrangement before the rate-determining step.

A cyclic (η^2-olefin)-Ni–CN transition state similar to the one drawn in Scheme 3 has previously been proposed for Lewis acid-assisted C–CN cleavage of Ni(0)-bound allyl cyanide.[3a] Table 4 also contains a list of $\Delta G^‡$ values for the system, calculated at 40 °C. All four values lie within a 1 kcal mol^{-1} range between the barriers for C–C bond cleavage (22.71 kcal mol^{-1}) and C–C bond formation (23.75 kcal mol^{-1}), demonstrating that all reaction pathways available to **1** are similar in energy.

C–C Activation of 1 with BPh₃. As described above, attempts to increase the concentration of C–C relative to C–H activation products by adjusting the reaction temperature of **1** met with limited success. Therefore, a strategy involving Lewis acids was applied to shift the reactivity of **1** toward C–C cleavage. Previously, DuPont researchers reported that, although C–C activation of allyl cyanide by [P(O-*o*-tol)₃]₃Ni at room temperature is very slow, reactions containing Lewis acids such as AlCl₃ and ZnCl₂ proceed instantaneously on mixing to give the π-allyl Ni(II)CN–Lewis acid adducts shown in eq 5.[8] Stabilization of the transition state **C** by the electron-withdraw-

ing Lewis acid was proposed to lower the barrier to C–CN cleavage, accounting for the rate acceleration observed.[3a] We investigated the reaction of **1** with the Lewis acid BPh₃ and found that this Lewis acid similarly facilitates C–C cleavage and completely suppresses C–H activation.

$$\text{(5)}$$
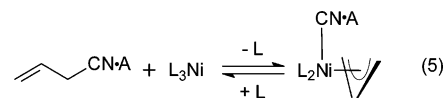
When 1 equiv of crystalline BPh₃ was added to a solution of **1** in THF-d_8 at −78 °C under inert atmosphere, the Lewis acid remained largely undissolved. However, a ^{31}P NMR spectrum of the reaction mixture collected at −50 °C revealed resonances for both **1** (73%) and a new singlet at 84.2 ppm (27%). In the ^{1}H NMR spectrum, the BPh₃ resonances integrated for about 0.25 equiv with respect to dippe and were shifted upfield from their positions in the free Lewis acid. The BPh₃ was then dissolved by warming the NMR tube to −30 °C and shaking. A −30 °C ^{31}P NMR spectrum collected immediately afterward showed quantitative conversion of **1** to the species displaying a singlet at 84.2 ppm, which was assigned as the Lewis acid adduct of C–C cleavage product **3**, (dippe)Ni(π-allyl)(C≡N–BPh₃) (**4**) (eq 6).

$$\text{(6)}$$
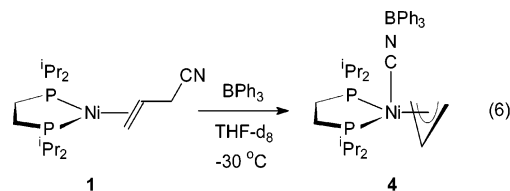
Characterization of the Ni(II) π-Allyl Cyanide–BPh₃ Adduct 4. Fluxional behavior was observed in the ^{1}H NMR spectrum of **4** at −30 °C (vide infra), but on warming the solution to 20 °C all ^{1}H resonances became sharp. No free BPh₃ appeared in the spectrum; instead, all BPh₃ resonances were shifted upfield by 0.3 (*para*-H) to 0.5 (*ortho*-H) ppm, consistent with coordination of the Lewis acid to the Ni-bound cyano group of **4**. Resonances for a π-allyl ligand undergoing rapid $\pi-\pi$ allyl interconversion, similar to those observed for **3** but shifted downfield by 0.16−0.18 ppm, also appeared in the spectrum. A quintet of triplets at 4.89 ppm ($J_{\text{H–H}}$ = 9.2 Hz, $J_{\text{H–P}}$ = 2.4 Hz, 1H) was assigned to the methine proton of the π-allyl ligand, while the *syn* and *anti* protons together yielded a slightly broadened doublet at 3.15 ppm ($J_{\text{H–H}}$ = 7.2 Hz, 4H). Two sets of doublets of doublets, shifted slightly upfield (<0.1 ppm) from their positions in the spectrum of **3**, were observed for the methyl groups on the dippe ligand.

The identity of **4** was confirmed by independent synthesis (eq 7). Addition of THF solvent at −78 °C to a mixture of **3** and 1 equiv of BPh₃, followed by slow warming to −20 °C, produced a homogeneous orange solution of **4**. Evaporation of the solvent and recrystallization of the residue from toluene at −30 °C afforded orange crystals suitable for X-ray diffraction. The structure of **4** is shown in Figure 4, and selected bond lengths and angles for the complex are given in Table 2. Like **3**, species **4** is square pyramidal with the C≡N–BPh₃ ligand in the axial position.[16] The Ni–C–N–B linkage is nearly linear, as has been reported for structurally characterized M–CNBPh₃
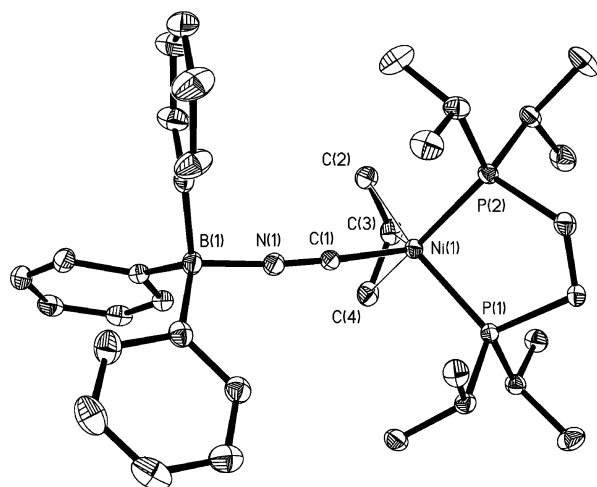
Figure 4. ORTEP drawing of **4** showing 30% probability ellipsoids.

complexes of Fe,[27] Ru,[28] Mn,[29] and Rh[30] (M−C−N and C−N−B angles range from 169° to 179°). The N−B bond length of 1.592(2) Å lies within the range documented for these complexes (1.575−1.608 Å), as does the C≡N bond length of 1.1517(19) Å (range = 1.135−1.163 Å). The C≡N bond of **4** is slightly longer than that of **3**, as was also reported for (Ph$_3$P)$_3$-RhCNBPh$_3$ as compared to (Ph$_3$P)$_3$RhCN,[30] although this trend is not consistent with the ν_{CN} shift observed for **4** versus **3** in the IR (vide infra). As in **3**, the π-allyl group of **4** is symmetrically bonded to Ni, with Ni−C and allyl C−C bond lengths nearly identical to those of **3** (Table 2).
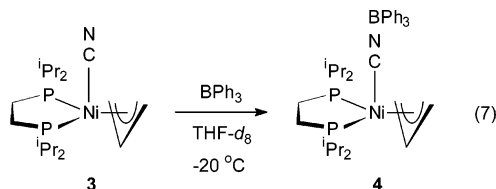
The IR spectrum of **4** in THF contains a C≡N stretching band at 2150 cm^{-1}, 54 cm^{-1} higher in energy than ν_{CN} for **3** (2096 cm^{-1}). Similar-magnitude increases in ν_{CN} have been reported on coordination of BPh$_3$ to the Ni-bound cyano group of [P(O-o-tol)$_3$]$_3$Ni(H)(CN) (56 cm^{-1} shift, from 2128 to 2184 cm^{-1})[3b,8] and on coordination of ZnCl$_2$ to [P(O-o-tol)$_3$]$_2$Ni(1-methyl-π-allyl)CN (42 cm^{-1} shift, from 2168 to 2210 cm^{-1}).[3a] Increases of 46−72 cm^{-1} in the C≡N stretching frequency are also well-documented on coordination of BPh$_3$ to M−CN (M = Fe, Ru, Mn, Pd)[31] and are attributed to the fact that the N lone pair on the metal-bound cyano group is antibonding in nature. Coordination of a Lewis acid to this lone pair removes electron density from CN antibonding orbitals, which strength-
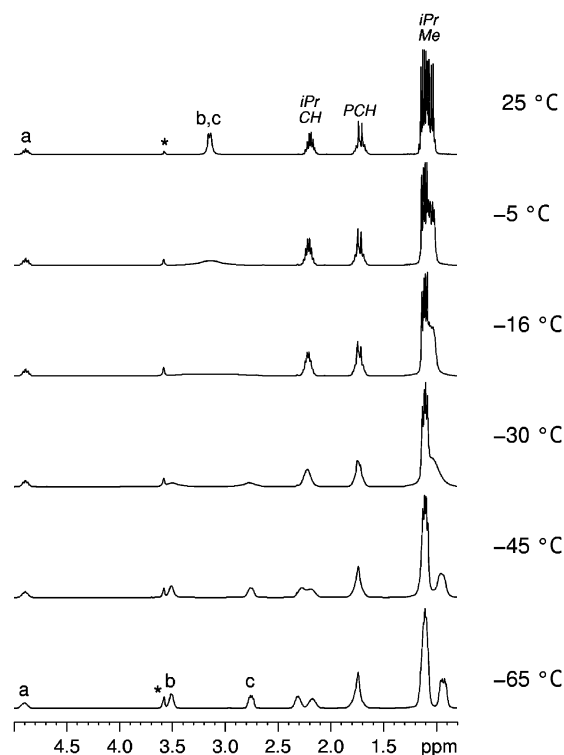
(27) (a) Almeida, S. S. P. R.; da Silva, M. F. C. G.; da Silva, J. J. R. F.; Pombeiro, A. J. L. *J. Chem. Soc., Dalton Trans.* **1999**, 467−472. (b) Laing, M.; Kruger, G.; Du Preez, A. L. *J. Organomet. Chem.* **1974**, *82*, C40−C42. (c) Ginderow, D. *Acta Crystallogr., Sect. B* **1980**, *36*, 1950−1951. (d) Amrhein, P. I.; Lough, A. J.; Morris, R. H. *Inorg. Chem.* **1996**, *35*, 4523−4525.
(28) Rocchini, E.; Rigo, P.; Mezzetti, A.; Stephan, T.; Morris, R. H.; Lough, A. J.; Forde, C. E.; Fong, T. P.; Drouin, S. D. *J. Chem. Soc., Dalton Trans.* **2000**, 3591−3602.
(29) Bellamy, D.; Connelly, N. G.; Hicks, O. M.; Orpen, A. G. *J. Chem. Soc., Dalton Trans.* **1999**, 3185−3190.
(30) Fernandes, M. A.; Circu, V.; Weber, R.; Varnali, T.; Carlton, L. *J. Chem. Crystallogr.* **2002**, *32*, 273−278.
(31) (a) Ermi, J.; Györi, B.; Bakos, A.; Czira, G. *J. Organomet. Chem.* **1976**, *112*, 325−331. (b) Pankowski, M.; Bigorgne, M. *J. Organomet. Chem.* **1983**, *251*, 333−338. (c) Haines, R. J.; Du Preez, A. L. *J. Organomet. Chem.* **1975**, *84*, 357−367. See also refs 6b, 27a, 28, and 29.

**Figure 5.** Dynamic ^{1}H NMR spectra of **4** in THF-d_8 (* = residual solvent).

ens the C≡N bond.[27a,31b] This effect should also shorten the C≡N bond, but no decrease in C−N bond distance was observed by X-ray crystallography.

^{13}CN-labeled **4** was prepared from ^{13}CN-labeled **3**, and its ^{13}C{^{1}H} NMR spectrum was collected at −20 °C. A triplet resonance ($^2J_{C-P}$ = 12.1 Hz) at 156.4 ppm, similar to the ^{13}CN resonance of **3** but shifted downfield by 1.6 ppm, was observed for the labeled cyano carbon, consistent with the 1.8 ppm downfield shift noted for the CN of *trans*-[FeH(CN)(dppe)$_2$] on coordination of BPh$_3$.[27a] Both allyl carbon resonances of **4** are shifted downfield of their analogues in **3**, just as the allyl proton resonances of **4** are shifted downfield in the ^{1}H NMR spectrum (Table 1).

Dynamic ^{1}H NMR spectroscopy of **4** in THF-d_8 (Figure 5) revealed that $\pi-\sigma$ allyl interconversion is less facile in this complex than in the non-BPh$_3$ analogue **3**. Like **3**, complex **4** undergoes rapid $\pi-\sigma$ allyl interconversion at room temperature, equilibrating the *syn* (H$_b$) and *anti* (H$_c$) protons of the allyl group. As the temperature is lowered, the H$_b$/H$_c$ doublet at 3.15 ppm broadens and separates into a pair of doublets at 3.51 (H$_b$) and 2.76 ppm (H$_c$). These protons coalesce at a much higher temperature in **4** (−16 °C) than in **3** (−68 °C), however, and the barrier to $\sigma-\pi$ allyl interconversion calculated for **4** at this temperature ($\Delta G^\ddagger$ = 11.7 kcal mol^{-1}) is ∼2.5 kcal mol^{-1} larger than $\Delta G^\ddagger$ for **3** at −68 °C.[16] Decreasing the temperature of **4** also results in separation of the dippe methine resonance at 2.20 ppm into two multiplets, and separation of the two dippe methyl resonances, each a doublet of doublets at 25 °C, into four (although three of these are coincident at 1.1 ppm; Figure 5). These data indicate that **4** possesses only a "vertical" mirror plane of symmetry (containing Ni−C−N−B and the allyl methine carbon, in the plane of the paper for **4** in eq 8) at the low-temperature limit and that the axial position of the cyanide

ligand renders the two ^{i}Pr groups on each P inequivalent.[32] At the high-temperature limit, however, an additional "horizontal" plane of symmetry coincident with the P–Ni–P plane, proposed to arise from rapid interconversion of "CNBPh$_3$ up" and "CNBPh$_3$ down" conformers of **4** via movement of the CNBPh$_3$ group into the P–Ni–P plane when the allyl group is σ-bound, must be present (eq 8). This σ–π allyl interconversion mechanism is analogous to that proposed for **3**[16] except for the slightly higher barrier to interconversion in **4**, which reflects the electronic effects of BPh$_3$ coordination to CN.

(8)

4
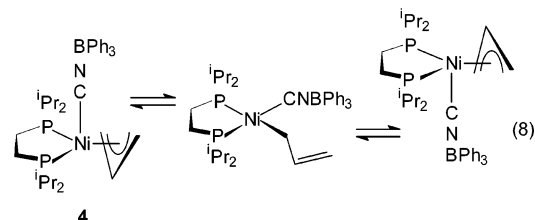
Abstraction of Cyanide from 4 by BPh$_3$. On standing at room temperature in THF-d_8 solution, isolated orange crystals of **4** were slowly converted to a new species (**5**) that appeared as a singlet at 79.5 ppm in the ^{31}P NMR spectrum of the reaction mixture (eq 9). After 42 days, ^{31}P NMR spectroscopy showed that a 1:1 mixture of **4** and **5** had been obtained. In the ^{1}H NMR spectrum, slightly broadened resonances for **4** were accompanied by broad resonances of **5** for the *syn* and *anti* protons of a π-allyl group undergoing π–σ allyl interconversion at a rate similar to the time scale of the ^{1}H NMR experiment (estimated $\Delta G^{\ddagger} = 14.8$ kcal mol^{-1} at +60 °C; see Supporting Information). After 90 days, a 1:2.8 mixture of **4** and **5** was attained.

(9)

4   **5**
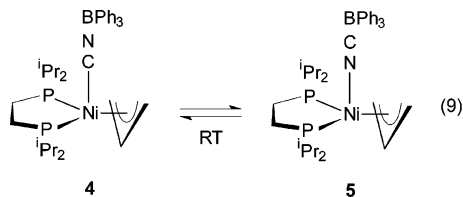
The same species **5** was also observed on addition of a 1:1 mixture of allyl cyanide and BPh$_3$ (1 equiv of each per Ni center) in THF-d_8 solution to [(dippe)Ni(μ-H)]$_2$ at room temperature. A 2:1 mixture of **4** and **5** was observed by ^{31}P NMR spectroscopy, and broad resonances for the fluxional species **5** again appeared in the ^{1}H NMR spectrum. Upon heating at 55 °C, **5** grew in at the expense of **4** until a 1:4 equilibrium ratio of **4** to **5** was reached. A second equivalent (per Ni center) of BPh$_3$ was then added to the reaction in an attempt to shift the **4** ⇌ **5** equilibrium toward **5** (Scheme 4). A ^{31}P NMR spectrum of the reaction mixture showed, however, that **4** was completely converted to a species displaying a singlet at 83.0 rather than 79.5 ppm. In the ^{1}H NMR spectrum, a set of sharp resonances that coincide with the resonances of the Ni(II) cation [(dippe)-Ni(π-allyl)]$^+$,[33] the precursor used to prepare **3**,[16] were observed instead of the broad resonances associated with **5**. In particular,

---

(32) Note that the diastereotopic methyl groups of each ^{i}Pr unit are always magnetically inequivalent, so at least two types of methyl groups will be observed in even the most symmetric (dippe)Ni complex. Also, the low-temperature NMR data do not allow differentiation between fast or slow rotation of the π-allyl group, although low-temperature data for **6** (vide infra) suggest that π-allyl rotation does not occur.

(33) Tenorio, M. J.; Puerta, M. C.; Salcedo, I.; Valerga, P. *J. Chem. Soc., Dalton Trans.* **2001**, 653–657. See also ref 16 for important ^{1}H NMR data.

Scheme 4
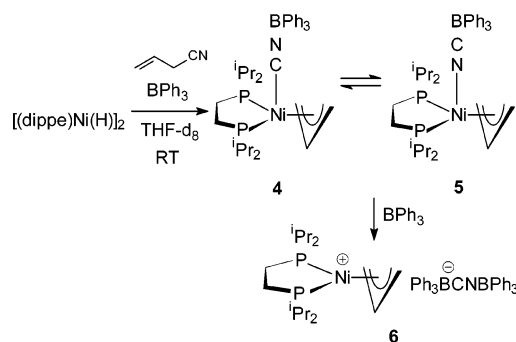
the appearance of separate, sharp doublet resonances at 4.40 ($J_{H-H} = 7.2$ Hz) and 2.43 ($J_{H-H} = 14.4$ Hz) ppm for the *syn* and *anti* protons of the allyl group clearly indicated that σ–π allyl interconversion does not occur at ambient temperature in this new species (**6**), unlike in **5**. Two new sets of BPh$_3$ resonances, different from the single set observed for **5**, also appeared in the aromatic region of the spectrum. Slow diffusion of pentane into the reaction mixture yielded a yellow crystal suitable for X-ray diffraction, which revealed that **6** consists of a (dippe)Ni(π-allyl) cation paired with the very bulky, noncoordinating anion [Ph$_3$BC≡NBPh$_3$]$^-$. The identity of **6** was confirmed by adding 2 equiv of BPh$_3$ to a red THF solution of **3** (eq 10). The reaction solution turned pale yellow immediately on mixing, and NMR spectra identical to those of **6** were observed for the reaction product.

(10)

3   **6**
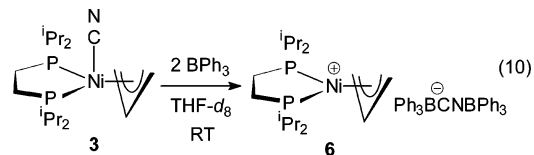
Species **5** was not isolated, because it was always produced as part of an equilibrium mixture with **4**, but is assigned as the complex (dippe)Ni(π-allyl)(N≡C–BPh$_3$) in which the cyanide has reversed its coordination geometry. A plausible mechanism for conversion of **4** to **5** involves dissociation of the [Ph$_3$BN≡C]$^-$ ligand from the Ni center of **4**, followed by migration of BPh$_3$ from N to C to give the carbon-bound Lewis acid adduct [Ph$_3$BC≡N]$^-$, followed by reattachment to the metal center. Migration of BPh$_3$ between the C and N termini of a cyanide ligand has previously been reported to convert M–N≡CBPh$_3$ to its linkage isomer M–C≡NBPh$_3$ (M = Pt,[34] Rh,[35] Ru[31c]) at elevated temperatures. In these cases, movement of BPh$_3$ from C to N is thermodynamically preferred because it allows cyanide coordination to the metal via a stronger M–C rather than a weaker M–N σ bond; in the present case, movement in the opposite direction suggests that the M–N complex **5** is more thermodynamically stable than the M–C complex **4**. The N–B bond of C≡NBPh$_3$ has also been reported to be significantly more labile than the C–B bond of N≡CBPh$_3$,[35] which may kinetically favor conversion of the N–B to the C–B isomer. Formation of **6** in the presence of 2 equiv of BPh$_3$ presumably occurs by trapping [Ph$_3$BN≡C]$^-$ with a second equivalent of Lewis acid as soon as it dissociates from Ni. The rapid rate of

---

(34) Manzer, L. E.; Anton, M. F. *Inorg. Chem.* **1977**, *16*, 1229–1231.

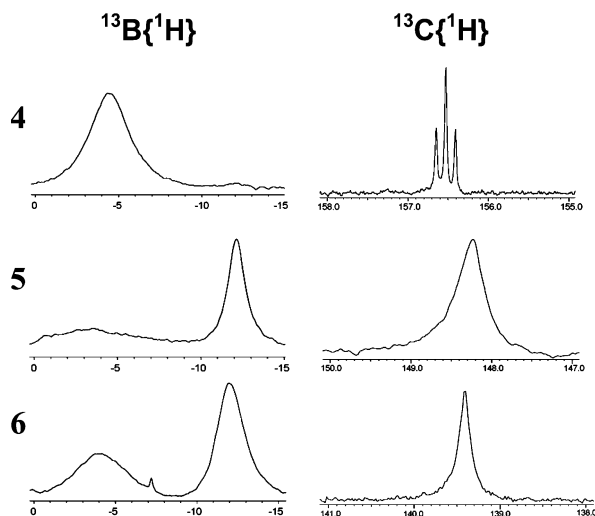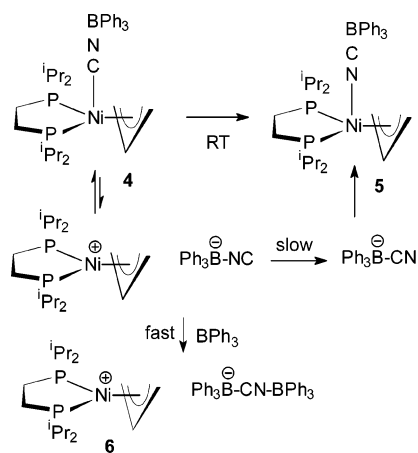(35) Carlton, L.; Weber, R. *Inorg. Chem.* **1996**, *35*, 5843–5850. See also ref 30.

Figure 6. $^{11}B\{^1H\}$ and $^{13}C\{^1H\}$ NMR spectra of **4**, **5**, and **6**.

Scheme 5

Figure 7. ORTEP drawing of **6** showing 30% probability ellipsoids. Note that C1 and N1 are disordered and the B−C−N−B unit is refined in both orientations using the Shelx SAME instruction.

boron resonances upon coordination of $B(C_6F_5)_3$ to the nitrogen as opposed to the carbon of a cyanide ligand.[36]

Characterization of the [(Ph₃B)₂CN]⁻ Anion and Ni(II) π-Allyl Cation of 6. The X-ray structure of **6** is shown in Figure 7. The bulky [Ph₃BC≡NBPh₃]⁻ counterion of **6** was previously prepared by Lippard and was characterized by X-ray crystallography in conjunction with a Mo cation.[37] In Lippard's structure, disorder of the anion across a center of symmetry in the crystal precluded resolution of the cyano C and N atoms, so composite half-carbon, half-nitrogen atoms were used in the refinement, yielding an average B−N/B−C bond distance of 1.603 Å. Similar disorder was encountered in the anion of **6**, which was modeled as a 50/50 mixture of B1−C−N−B2 and B1−N−C−B2 isomers. Note that the average of these four B−N and B−C bond distances is 1.605 Å, in excellent agreement with the value obtained by Lippard.[37] The structure of $[(C_6F_5)_3BC≡NB(C_6F_5)_3]^-$, an even more weakly coordinating anion developed for metallocene polymerization catalysts, has also been determined.[38] Surprisingly, the B−C distance in the perfluorinated anion is about 0.3 Å longer than the B−C distances of **6**, despite the electron-withdrawing influence of the fluoroaryl groups, while the B−N distance is shorter than in **6**. The B−N bond distance of **4** is also shorter than the average B−N distance in **6** (Table 2).

The structure of the (dippe)Ni(π-allyl) cation of **6** is similar to that of the closely related analogue [(dippe)Ni(π-2-methylallyl)]⁺.[33] Also, shorter Ni−C and Ni−P bond distances are observed for **6** than for **3** or **4**, in accord with the increased charge on the metal center (Table 2). The IR spectrum of **6** in THF contains a C≡N stretching band at 2245 cm⁻¹, in good agreement with the value of 2255 cm⁻¹ reported for Lippard's Mo salt (KBr pellet).[37]

The ^{13}CN-labeled analogue of **6** was prepared from ^{13}CN-labeled **3**, and a room-temperature $^{13}C\{^1H\}$ NMR spectrum revealed a large, broad (56 Hz width at half-height) resonance at 139.3 ppm for the labeled ^{13}CN of **6**. The resonance sharpens

6 formation from **3** thus implies that BPh₃ migration, rather than dissociation of [Ph₃BN≡C]⁻, is the rate-determining step in the slow transformation of **4** to **5** (Scheme 5). Finally, the lower barrier to σ−π allyl interconversion observed for **5** relative to **6** suggests that the [Ph₃BC≡N]⁻ ligand of **5** interacts more weakly with the Ni(II) center than the [Ph₃BN≡C]⁻ ligand.

Further evidence for the formulation of **5** as the N-bound isomer (dippe)Ni(π-allyl)(N≡C−BPh₃) comes from comparison of the $^{11}B\{^1H\}$ and $^{13}C\{^1H\}$ NMR spectra of **4**, **5**, and **6** (Figure 6). The initial adduct **4** formed from reaction of **1** or **3** with BPh₃ shows a broad ($\nu_{1/2} \approx 3$ ppm) downfield singlet in the ^{11}B NMR spectrum due to coordination of boron to the quadrupolar nitrogen of the cyanide ligand. The ^{13}C NMR spectrum shows a sharp triplet ($J = 12.1$ Hz) for the carbon attached to nickel coupling to two equivalent phosphorus nuclei. Isomer **5**, however, shows a sharp singlet ($\nu_{1/2} \approx 1$ ppm) shifted to higher field in the ^{11}B NMR spectrum, as the boron is now bound to carbon. The ^{13}C spectrum now shows a broad resonance ($\nu_{1/2} \approx 0.5$ ppm) for the cyano carbon bound to quadrupolar boron. As a comparison, salt **6** shows both broad and narrow singlets in the ^{11}B NMR spectrum, because two kinds of boron are present, one in each environment, and a slightly broadened singlet in the ^{13}C NMR spectrum. A recent publication by Green et al. shows several examples of metal−cyanide complexes that display downfield shifts and broadened
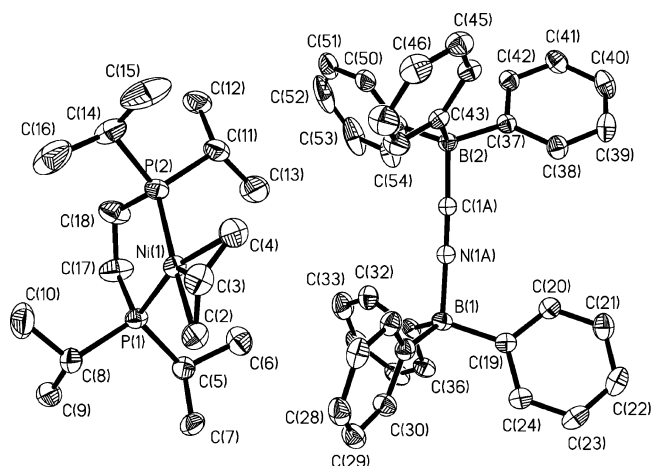
(36) Vei, I. C.; Pascu, S. I.; Green, M. L. H.; Green, J. C.; Schilling, R. E.; Anderson, G. D. W.; Rees, L. H. *Dalton Trans.* **2003**, 2550−2557.
(37) Giandomenico, C. M.; Dewan, J. C.; Lippard, S. J. *J. Am. Chem. Soc.* **1981**, *103*, 1407−1412.
(38) (a) Lancaster, S. J.; Walker, D. A.; Thornton-Pett, M.; Bochmann, M. *Chem. Commun.* **1999**, 1533−1534. (b) Zhou, J.; Lancaster, S. J.; Walker, D. A.; Beck, S.; Thornton-Pett, M.; Bochmann, M. *J. Am. Chem. Soc.* **2001**, *123*, 223−237.
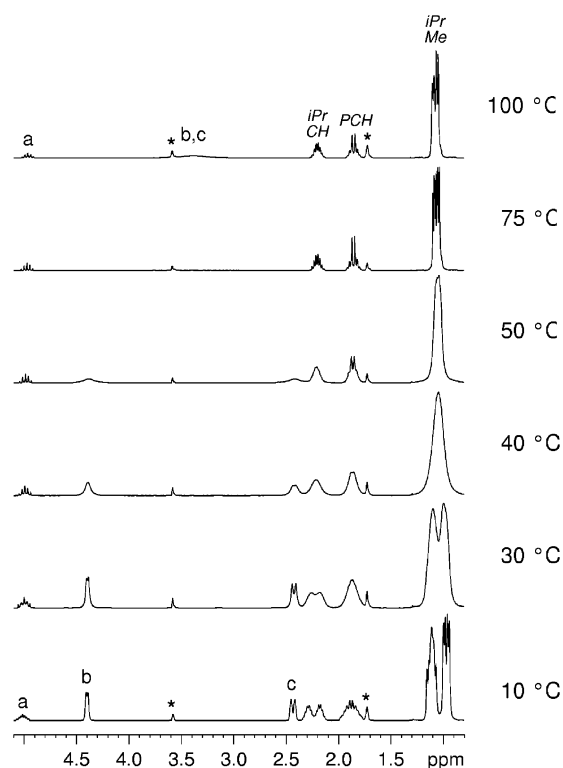
**Figure 8.** Dynamic ^{1}H NMR spectroscopy of **6** in THF-d_8 (* = residual solvent).

and shifts upfield by ~4 ppm at −50 °C, consistent with quadrupolar line broadening. Resonances for the methine and terminal allyl carbons were identified at 117.1 and 64.7 ppm, significantly downfield of their counterparts in **3** and **4**.

Dynamic ^{1}H NMR spectroscopy of **6** in THF-d_8 (Figure 8) revealed that π–σ allyl interconversion is slow for this complex at room temperature, unlike for **3** and **4**. However, spectra of **4** and **6** at the low-temperature limit are similar in that both contain two ^{i}Pr methine and four ^{i}Pr methyl resonances (overlapping one another in **6**), indicating that the two ^{i}Pr groups on each P of dippe are inequivalent (neither complex possesses a "horizontal" mirror plane of symmetry, vide supra). Because no apical ligand is present in **6** to lower the symmetry of the complex, the "horizontal" mirror plane must be absent because the π-allyl group does not rotate at this temperature. As π–σ allyl interconversion becomes rapid at higher temperatures, the methine protons coalesce into a single resonance and the methyl groups coalesce into two nearly coincident doublets of doublets, consistent with the behavior observed for **3** and **4**. Doublets at 4.40 and 2.43 ppm for the *syn* (H$_b$) and *anti* (H$_c$) protons of **6** also broaden and coalesce (at 75 °C) into a single resonance at about 3.38 ppm, although the high-temperature limit could not be reached due to solvent boiling point limitations. Calculation of the barrier for π–σ allyl interconversion in **6** yielded $\Delta G^{\ddagger}$ = 15.9 kcal mol^{-1}, significantly higher than in **4** (11.7 kcal mol^{-1}) or **3** (9.3 kcal mol^{-1}), and slightly higher than in **5** (14.8 kcal mol^{-1}).

The difficulty of π–σ allyl isomerization in **6** as compared to **3** or **4** indicates that movement of the cyano ligand into the P$_2$Ni square plane during the interconversion speeds up the process considerably, perhaps through a mechanism in which the CN ligand effectively displaces one end of the π-allyl group from Ni. Consistent with this interpretation, the fact that the

barrier to σ–π allyl interconversion for **4** is higher than for **3** but lower than for **6** implies that the CNBPh$_3$ ligand of **4** is less strongly coordinated to Ni than the CN ligand of **3**, and therefore less good at stabilizing the square planar σ-allyl isomer (eq 8). In fact, weakening of the Pt–C bond of a Pt(CN) complex upon coordination of BPh$_3$ to the cyano group's nitrogen atom has previously been documented, lending support to this analysis.[39] Observation of a barrier to σ–π allyl interconversion for **5** higher than for **4**, yet lower than for **6**, likewise suggests that the [Ph$_3$BC≡N]$^-$ ligand of **5** interacts weakly with the Ni center, more than in the completely noncoordinating [Ph$_3$BC≡NBPh$_3$]$^-$ counterion of **6**, although less than the [Ph$_3$BN≡C]$^-$ ligand of **4**.

Preparation and Decomposition of the Ni(0) Crotononitrile–BPh$_3$ Adducts 7. As described above, C–C activation product **4** is the only species observed when 1 equiv of BPh$_3$ reacts with **1**; no traces of the BPh$_3$ adduct of **1** or BPh$_3$-coordinated counterparts of the C–H activation products **2** were detected (eq 6). To test whether **4** is the thermodynamic or kinetic product of the reaction of **1** with BPh$_3$, the BPh$_3$-coordinated crotononitrile complexes *trans*- and *cis*-**7** were prepared by addition of BPh$_3$ to **2** (eq 11). A ^{31}P NMR spectrum of the reaction products consisted of two sets of doublets, at 71.8 and 69.1 ppm with $^2J_{P-P}$ = 44 Hz for *trans*-**7**, and at 71.8 and 68.7 ppm with $^2J_{P-P}$ = 44 Hz for *cis*-**7**. Isolated yellow crystals (vide infra) of *trans*- and *cis*-**7** were heated to 55 °C in THF-d_8 solution to investigate whether **7** equilibrates with **4**, but no conversion to **4** was observed (eq 11); at 80–100 °C, traces of **4** were detected along with many unidentified decomposition products. These results demonstrate that **4** and **7** do not interconvert under the reaction conditions for eq 6 (−30 °C), making **4** the kinetic product of the reaction of **1** with BPh$_3$. Thus, C–CN cleavage of Ni(0)-coordinated allyl cyanide is both faster than C–H bond activation and effectively irreversible in the presence of BPh$_3$, in marked contrast to the non-BPh$_3$ reaction.
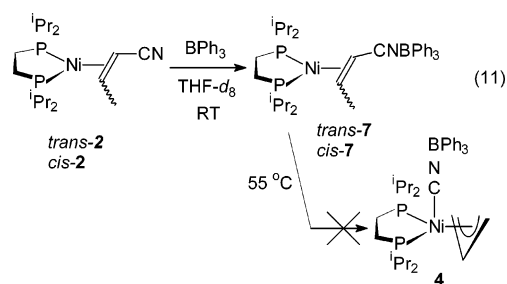
Characterization of the Ni(0) Crotononitrile–BPh$_3$ Adducts 7. In the ^{31}P NMR spectrum of **7**, the 10 Hz decrease in P–P coupling constant as compared to **2** (Table 1) suggests that the Lewis acid-coordinated olefin of **7** binds more strongly to Ni(0) than does the olefin of **2**, perhaps because it can accept more π-electron donation from Ni. The room-temperature ^{1}H NMR spectrum of **7** is similar to that of **2**, with the addition of BPh$_3$ resonances shifted upfield from their positions in the free Lewis acid, consistent with BPh$_3$ coordination to crotononitrile. As in spectra of **2**, resonances for the olefin protons of crotononitrile could not be distinguished from those of the four inequivalent methine protons of dippe, but all dippe and

(39) Manzer, L. E.; Parshall, G. W. *Inorg. Chem.* **1976**, *15*, 3114−3115.
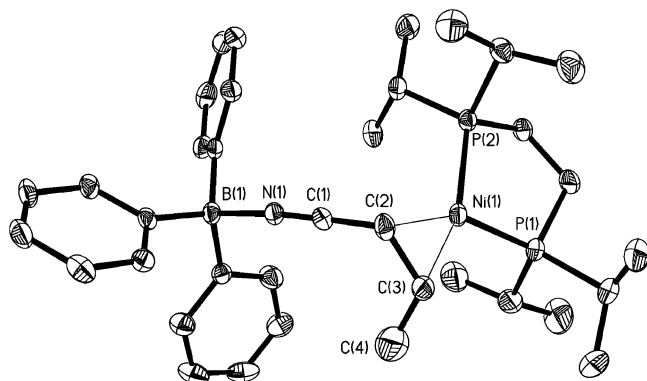
Figure 9. ORTEP drawing of *cis*-**7** showing 30% probability ellipsoids.

crotononitrile resonances appear upfield of 2.71 ppm (Table 1),[11] consistent with η^2-olefin binding of the nitrile to Ni. Eight distinct resonances for the eight methyl groups of dippe were observed in the ^{1}H NMR spectrum, indicating that the Lewis acid-coordinated olefin of **7** (like the olefin of **2**) does not rotate at room temperature.

Recrystallization from THF/pentane yielded a crystal of *cis*-**7** whose X-ray structure was determined (Figure 9). Selected bond lengths and angles for the complex are given in Table 2. The structure of *cis*-**7** is square planar, with all of the atoms in the C4−C3−C2−C1−N−B unit lying approximately in a plane perpendicular to the P$_2$Ni plane. The C2−C1−N−B linkage is nearly linear, although the bulky BPh$_3$ group bends slightly away from the ^{i}Pr groups of the dippe ligand. The N−B bond in *cis*-**7** is longer than the corresponding bond in **4**, but shorter than the N−B distance in **6**. Surprisingly, coordination of BPh$_3$ to crotononitrile does not alter the C≡N or C=C bond lengths of the ligand. The only difference between the (dippe)Ni(crotononitrile) cores of **2** and **7** is that the olefin is bound slightly less symmetrically to Ni(0) in *cis*-**7** than in *trans*-**2**, with Ni−C1 and Ni−C2 bond distances of 1.961(4) Å for the carbon bound to CNBPh$_3$ and 1.933(4) Å for the carbon bound to the methyl group. Otherwise, coordination of BPh$_3$ to the crotononitrile ligand of **2** has remarkably little effect on the structure of the complex.

The IR spectrum of **7** (pure *cis*-, pure *trans*-, or a mixture) contains a single C≡N stretching band at 2244 cm^{-1}, 63 cm^{-1} higher in energy than that of **2** (Table 1). This increase upon Lewis acid coordination to Ni-bound crotononitrile is greater than the 54 cm^{-1} increase observed when BPh$_3$ coordinates to the Ni-bound cyano group of **3**, but smaller than the 74 cm^{-1} increase observed on coordination of BPh$_3$ to free crotononitrile (ν_{CN} shifts from 2221 to 2295 cm^{-1}). Comparison of the C≡N stretching frequency of **7** to that of free crotononitrile also reveals that the two substituents bound to crotononitrile in **7**, the π-electron-withdrawing Lewis acid BPh$_3$ and the π-electron-donating Lewis base (dippe)Ni(0), exert opposite but roughly equal electronic effects on cyano bond strength, leaving Ni complex **7** with a C≡N bond slightly stronger than that of the free nitrile.

In the ^{13}C{^{1}H} NMR spectrum of *cis*-**7**, the carbon resonance of the BPh$_3$-coordinated cyano group is shifted 1.7 ppm upfield from ^{13}CN of *cis*-**2** (Table 1). The =C(H)CH$_3$ carbon also shifts upfield by 1.0 ppm for *cis*-**7** and 1.7 ppm for *trans*-**7**, while the =C(H)CNBPh$_3$ carbon apparently resonates at the same fre-

quency as in **2** for both *trans*- and *cis*-**7**.[40] By contrast, resonances for both olefin carbons and the cyano carbon of Lewis acid adduct **4** are shifted downfield from their positions in the non-BPh$_3$ analogue **3**.

Summary and Conclusions

The reaction of [(dippe)Ni(μ-H)]$_2$ with allyl cyanide at low temperature cleanly produces the η^2-olefin complex (dippe)Ni-(CH$_2$=CHCH$_2$CN) (**1**). At ambient temperature or above, **1** is converted to a mixture of C−H cleavage products (dippe)Ni-(η^2-crotononitrile) (*cis*-**2** and *trans*-**2**) and the C−CN cleavage product (dippe)Ni(π-allyl)CN (**3**). At longer reaction times, **3** is completely converted to **2**, indicating that C−C cleavage is reversible and the Ni-olefin complexes **2** are more thermodynamically stable than the Ni(π-allyl) cyanide **3**.

The rates for the competitive C−H cleavage, C−C cleavage, and C−C bond formation reactions that occur in this system were determined as a function of temperature and showed that the rate constant for the C−CN bond formation step exhibited a much stronger temperature dependence than the rate constants for C−H and C−C cleavage. C−C activation becomes increasingly kinetically competitive with C−H activation at elevated temperatures, producing more **3**. The activation parameters for the cleavage and bond formation steps revealed that $\Delta H^{\ddagger}$ is much larger for C−CN formation than for C−C or C−H cleavage, while $\Delta S^{\ddagger}$ for C−CN coupling is positive rather than negative.

The reaction of **1** with BPh$_3$ at low temperature yields the C−C activation product (dippe)Ni(π-allyl)(CNBPh$_3$) (**4**) rapidly and exclusively, demonstrating that C−C activation of allyl cyanide is both faster than C−H activation and irreversible in the presence of the Lewis acid. This complex shows linkage isomerism of the cyano group bridging between the nickel and boron centers. Additional Lewis acid completely removes the cyanide as [Ph$_3$B−CN−BPh$_3$]$^-$. The (dippe)Ni(crotononitrile)−BPh$_3$ adducts **7**, analogues of the C−H activation products **2**, were not observed in the reaction of allyl cyanide with (dippe)-Ni(0) in the presence of BPh$_3$, but were prepared independently and characterized by X-ray crystallography, IR, and NMR spectroscopy. Conversion of **7** to the C−C cleavage product **4** was not observed, even at high temperatures, indicating that **4** is the kinetic product of the Lewis acid-assisted reaction of allyl cyanide with Ni(0).

The barriers to $\pi-\sigma$ allyl interconversion (determined from dynamic ^{1}H NMR experiments) for the π-allyl complexes studied lie in the order **3** < **4** < **5** < **6**. The presence of an axial ligand in the coordination sphere of Ni clearly facilitates $\pi-\sigma$ allyl interconversion, as it moves into the P$_2$Ni plane when the allyl ligand is σ-bound and stabilizes the σ-allyl conformer.

Experimental Section

General Methods. All reactions were performed under N$_2$ in a Vacuum Atmospheres glovebox or using standard Schlenk techniques. Allyl cyanide and crotononitrile (2:1 *cis:trans*) were purchased from Aldrich, degassed, purified by vacuum transfer, and stored in the glovebox over molecular sieves. BPh$_3$ was purchased from Aldrich, recrystallized from pentane or hexanes at −30 °C under inert atmosphere, dried in vacuo overnight, and stored in the glovebox.

(40) However, the chemical shifts for =*C*(H)CNBPh$_3$ given in Table 1 are probably not accurate because one-half of this resonance lies under the THF-*d*$_8$ resonance at 25.4 ppm; see ref 21.

(COD)₂Ni and Ph₃P=O were purchased from Aldrich and used as received. The ligand dippe[41] and the complexes [(dippe)Ni(μ-H)]₂[41] and (dippe)Ni(π-allyl)CN (**3**)[16] were prepared by literature protocols. All solvents, including THF-d_8, were distilled or vacuum transferred from Na/benzophenone and stored in the glovebox.

Routine room-temperature ³¹P{¹H} and ¹H NMR spectra were recorded on a Bruker AMX400 instrument; low- and high-temperature ³¹P{¹H}, ¹H, and ¹³C{¹H}NMR spectra were recorded on a Bruker Avance400 spectrometer. Chemical shifts are given in ppm and referenced to residual solvent peaks (¹H and ¹³C NMR) or to an external standard (85% H₃PO₄, ³¹P NMR). Complete spectra data are reported in the Supporting Information. IR spectra were recorded in THF solution on a Mattson Instruments 6020 GALAXY Series FT spectrophotometer. Crystallographic data were collected using a Siemens SMART diffractometer with CCD detection. Elemental analysis was performed by Complete Analysis Laboratories, Inc., Parsippany, NJ.

(dippe)Ni(η^2-C≡C−Allyl cyanide) (1). A small stir bar and a very dark red solution of [(dippe)Ni(μ-H)]₂ (15.6 mg, 24.2 μmol) in THF-d_8 were carefully added to a special NMR tube (made in-house, see Supporting Information) equipped with a sidearm and Schlenk adapter, while allyl cyanide (4.0 μL, 49.7 μmol) was added to the sidearm using a 10 μL syringe. The Ni solution and the allyl cyanide were cooled in separate acetone/dry ice baths, the tube was evacuated to degas both liquids, and the allyl cyanide was vacuum transferred into the Ni solution, which turned yellow-brown. The cold bath around the NMR tube was removed briefly (for <10 s) so that the reaction solution could be mixed by moving the stir bar up and down in the tube with a magnet. The reaction solution was degassed to remove H₂ (vigorous bubbling occurs), and was then stirred and degassed several more times until no more H₂ gas was evolved. The stir bar was drawn up into the sidearm with the magnet, and the NMR tube was flame sealed under vacuum beneath the sidearm. The tube was transferred directly from the −78 °C bath to the −30 °C NMR probe.

(dippe)Ni(η^2-C≡C−Crotononitrile) (2). A solution of dippe (191 mg, 0.73 mmol) in 15 mL of THF was added to crystalline yellow (COD)₂Ni (201 mg, 0.73 mmol), forming a yellow solution that was stirred for 30 min. The solvent was removed in vacuo, and the product (dippe)Ni(COD) was dried for 30 min to remove free COD. A solution of crotononitrile (75 mg, 1.12 mmol; 2:1 *cis:trans*) in 15 mL of THF was added to the reaction flask, giving a brownish-yellow solution that was stirred for 30 min. The solvent was removed in vacuo, and the residue was dried for 30 min; the ³¹P NMR spectrum of an aliquot showed that 6% (dippe)Ni(COD) remained. A solution of another 50 mg (0.74 mmol) of crotononitrile in 15 mL of THF was added to the reaction flask and stirred for 30 min. After removal of the solvent and drying for 30 min in vacuo, the ³¹P NMR spectrum of the yellow-brown oily residue showed complete conversion to **2** (58% *cis*:42% *trans*). Some of the residue was dissolved in (TMS)₂O and allowed to stand at −30 °C, yielding 114 mg of yellow microcrystals (42% *cis*: 58% *trans*-**2** by ³¹P NMR). The rest of the residue was dissolved in THF; slow diffusion of pentane into this solution at −30 °C yielded 47 mg of large, pale yellow crystals (97% *cis*:3% *trans*-**2** by ³¹P NMR; 57% total yield). IR (THF) ν_{CN} = 2181 cm⁻¹. Anal. Calcd for C₁₈H₃₇P₂-NNi: C, 55.70; H, 9.61; N, 3.61. Found: C, 55.64; H, 10.09; N, 3.61.

¹³CN-Labeled 2. Upon standing at room temperature for 112 h, a red solution of (dippe)Ni(π-allyl)¹³CN[16] in THF-d_8 slowly turned yellow. ³¹P{¹H} NMR spectroscopy revealed that the sample still contained 3% of the starting material along with the desired **¹³CN-2** (53% *cis*:47% *trans*), so it was heated to 55 °C for 1 h, producing a solution with <1% (dippe)Ni(π-allyl)¹³CN.

(dippe)Ni(π-Allyl)(CNBPh₃) (4). Red solid (dippe)Ni(π-allyl)CN (**3**; 26.0 mg, 67.0 μmol) and white solid BPh₃ (15.7 mg, 64.8 μmol) were combined in a 100 mL round-bottom flask equipped with a

Schlenk adapter, which was evacuated and cooled in a liquid N₂ bath. Next, 30 mL of dry, degassed THF was vacuum transferred into the reaction flask, and the reaction mixture was thawed in an acetone/dry ice bath and stirred. Neither reagent dissolved at −78 °C, so the bath was gradually warmed by removal of dry ice and addition of warm acetone until a homogeneous orange solution was obtained at −20 °C. The cold bath was removed, and the solvent was evaporated in vacuo as the mixture warmed gradually to room temperature. The orange powder obtained was recrystallized from toluene at −30 °C, yielding red-orange crystals that were dried in vacuo (22.0 mg, 54% yield). IR (THF) ν_{CN} = 2150 cm⁻¹. Anal. Calcd for C₃₆H₅₂P₂NBNi: C, 68.61; H, 8.32; N, 2.22. Found: C, 68.60; H, 8.57; N, 2.24.

¹³CN-Labeled 4. First, 0.6 mL of dry, degassed THF-d_8 was vacuum transferred from a Na/benzophenone still into an evacuated, liquid N₂-cooled NMR tube containing red solid (dippe)Ni(π-allyl) ¹³CN (25.8 mg, 66.3 μmol) and white solid BPh₃ (14.4 mg, 59.5 μmol). The reaction mixture was then thawed in an acetone/dry ice bath. The NMR tube was cooled thoroughly, and was then removed briefly from the bath and shaken several times until a homogeneous orange solution was obtained. The sample was warmed to room temperature, and a ³¹P{¹H} NMR spectrum taken immediately showed 77% **¹³CN-4**, 12% byproduct **¹³CN-6**, and 11% dippe oxide impurity. After removal of the solvent in vacuo, the resulting orange powder was recrystallized from toluene at −30 °C, yielding red-orange crystals that were dried in vacuo and found to be 97% pure by ³¹P NMR (3% **¹³CN-6**).

[(dippe)Ni(π-Allyl)]⁺[Ph₃BCNBPh₃]⁻ (6). A solution of BPh₃ (50.1 mg, 207 μmol) in 4−5 mL of THF was added to red solid (dippe)Ni-(π-allyl)CN (**3**; 40.2 mg, 104 μmol). Upon mixing, the reaction mixture turned from wine-red to pale yellow. Fluffy pale yellow solid precipitated immediately upon addition of 5 mL of pentane to the reaction mixture. The product was isolated by filtration and dried in vacuo (75.0 mg, 83% yield). Anal. Calcd for C₅₄H₆₇P₂NB₂Ni: C, 74.35; H, 7.74; N, 1.61. Found: C, 74.36; H, 7.73; N, 1.61.

¹³CN-Labeled 6. This was prepared in the same way as the nonlabeled analogue from 19.9 mg of (dippe)Ni(π-allyl)¹³CN (51.1 μmol) and 24.7 mg of BPh₃ (102 μmol); 32.6 mg of product was obtained (73% yield).

(dippe)Ni(η^2-C≡C−Crotononitrile−BPh₃): 97% *cis*-7. A yellow solution of 97% *cis*-**2** (18.2 mg, 46.9 μmol) in THF-d_8 was added to solid BPh₃ (11.4 mg, 47.1 μmol), producing a yellow solution. Quantitative conversion to *cis*-**7** was observed by ³¹P NMR. After evaporation of the solvent, the sample was redissolved in toluene and a couple drops of THF; slow diffusion of pentane into this solution at −30 °C produced pale yellow microcrystals (9.2 mg, 31% yield). IR (THF) ν_{CN} = 2244 cm⁻¹. Anal. Calcd for C₃₆H₅₂P₂NBNi: C, 68.61; H, 8.32; N, 2.22. Found: C, 68.63; H, 8.55; N, 2.31.

(dippe)Ni(η^2-C≡C−Crotononitrile−BPh₃): 94% *trans*-7. This was prepared in the same way as 97% *cis*-**2** using 59.0 mg of **2** (152 μmol, 42% *cis*:58% *trans*) and 36.4 mg of BPh₃ (150 μmol). Recrystallization from THF/pentane at −30 °C produced 40.9 mg of yellow microcrystals (70% *cis*:30% *trans* by ³¹P NMR), while a second crop obtained from the mother liquor yielded 15.0 mg of yellow needles that were 94% *trans*-**2** by ³¹P NMR (58% overall yield).

Dynamic ¹H NMR of 4 and 5. About 20 mg of orange crystalline **4** was added to a J. Young NMR tube, which was cooled in a liquid N₂ bath. Next, 0.5 mL of THF-d_8 was vacuum transferred from a Na/benzophenone still into the NMR tube, and the solution was thawed in an acetone/dry ice bath. The NMR tube was thoroughly cooled, and was then removed briefly from the bath and shaken until a homogeneous orange solution was obtained. ³¹P{¹H} and ¹H NMR spectra were recorded at 5 °C intervals between −70 and 50 °C. All ³¹P{¹H} NMR spectra consisted of a sharp singlet, which shifted progressively upfield as the temperature was raised [3.8 ppm difference between δ(−70 °C) and δ(50 °C)], while the ¹H NMR spectra varied with temperature as shown in Figure 5. Additional ¹H NMR spectra were collected at −16 and −17 °C to precisely identify the temperature at which the *syn* and

(41) Supporting Information from: Vicic, D. A.; Jones, W. D. *J. Am. Chem. Soc.* **1997**, *119*, 10855−10856.

anti protons on the terminal carbon of the π-allyl group coalesce (-16 °C). After several months, **4** converted to **5**, and another set of VT NMR spectra were recorded (see Supporting Information).

Dynamic ^{1}H NMR of 6. About 20 mg of pale yellow **6** was dissolved in 0.5 mL of THF-d_8 and was added to a J. Young NMR tube. ^{31}P{^{1}H} and ^{1}H NMR spectra were recorded at 10 °C intervals between -20 and 30 °C, at 5 °C intervals between 30 and 100 °C, and at 110 and 120 °C. All ^{31}P{^{1}H} NMR spectra consisted of a singlet that shifted progressively upfield as the temperature was raised [1.1 ppm difference between $\delta(-20$ °C) and $\delta(120$ °C)], while the ^{1}H NMR spectra varied with temperature as shown in Figure 8.

Distribution of Species Plots (Figure 1). Complex **1** was generated at low temperature in a special flame-sealed NMR tube as described above (see Supporting Information), except that Ph$_3$P=O was also added to the reaction as an internal standard, dissolved in THF-d_8 along with [(dippe)Ni(μ-H)]$_2$. ^{31}P and ^{1}H NMR spectra were recorded at -30 °C to verify the purity of **1**. The NMR tube was removed from the probe and returned to an acetone/dry ice bath, and the probe was warmed to the reaction temperature (20, 30, 35, 40, or 50 °C). The magnet was preshimmed at this new temperature using a "dummy" sample. The NMR tube was transferred directly from the dry ice/acetone bath into a water bath at the reaction temperature (the moment of transfer is considered the reaction start time, $t = 0$), where it was allowed to equilibrate for 10–15 s. The tube was transferred to the NMR probe, the shims were adjusted quickly, and a variable-delay kinetics program was initiated. The program collected ^{31}P NMR spectra over 3 (50 °C reaction) to 36 h (20 °C reaction). Integration of these spectra afforded the percents distribution of species **1**–**3**, which were plotted in Microsoft Excel as shown in Figure 1.

Two minor impurities, a broad singlet at ~78 ppm (1–2%) and a sharp singlet at 90.9 ppm ($\leq$5%), were also observed in the ^{31}P NMR spectrum of the reaction but are not included in Figure 1. The former was identified as (dippe)Ni(π-allyl)Cl by comparison of a mass spectrum of the reaction mixture to the mass spectrum of an authentic sample, generated by reaction of [(dippe)Ni(μ-H)]$_2$ with allyl chloride. The chloride ion needed to generate this side product is an impurity in the starting material [(dippe)Ni(μ-H)]$_2$ (prepared from (dippe)NiCl$_2$ and superhydride).[41] The δ 90.9 species disappeared from the reaction mixture concomitant with formation of pale yellow crystals in the NMR tube, which were identified by X-ray diffraction as the decomposition product (dippe)Ni(CN)$_2$.[42] This product has also been observed during C–CN cleavage reactions of (dippe)Ni(ArCN) complexes.[7]

Determination of Rate Constants via Simulation of Distribution of Species Plots. The mechanism shown in Scheme 2 and the experimental data for one reaction temperature were input into the program KINSIM.[22] Values for the rate constants k_1, k_{-1}, k_2, and k_3 were entered manually, a simulation was performed, and the calculated concentration versus time curves were superimposed on the experimental data. The goodness of fit was evaluated by eye, and the rate constant values were adjusted until a reasonable fit of calculated to experimental data was obtained. The output from KINSIM was then input into the program FITSIM,[22] which used a nonlinear regression analysis method to vary the rate constants until the best fit to the experimental data was obtained. The output of FITSIM included the rate constants and their standard deviations σ (Table 3), as well as calculated concentration versus time data, which was plotted along with

the experimental data in Microsoft Excel (Figure 1; smooth lines; see also Supporting Information).

Formation of 4 from 1 and BPh$_3$ at Low Temperature. A small stir bar and a very dark red solution of [(dippe)Ni(μ-H)]$_2$ (15.9 mg, 24.7 μmol) in THF-d_8 were added to a special NMR tube equipped with a sidearm and Schlenk adapter (see Supporting Information), and solid BPh$_3$ (11.9 mg, 49.1 μmol) was added to the sidearm. A THF-d_8 solution of allyl cyanide (5.0 μL, 62.2 μmol) was vacuum distilled into the tube, turning the Ni solution yellow-brown. The reaction solution was mixed and degassed as described above for **1**, until no more H$_2$ was evolved. The solution was then frozen in liquid N$_2$, and the NMR tube was removed from the Schlenk line and tilted so that the BPh$_3$ in the sidearm fell into the tube. The reaction mixture was thawed in an acetone/dry ice bath, but only some of the solid dissolved at -78 °C, even after mixing with the stir bar. The stir bar was drawn up into the sidearm with the magnet, and the NMR tube was flame sealed under vacuum below the sidearm. The tube was transferred directly from the -78 °C bath to the -50 °C NMR probe. ^{31}P and ^{1}H NMR spectra were collected at -50 and -30 °C; the sample was then removed from the probe, shaken once so that the BPh$_3$ dissolved, and returned to the probe. Further spectra were collected at -30, -10, and 20 °C, as described in the text.

Formation of 5 and 6 from [(dippe)Ni(μ-H)]$_2$, Allyl Cyanide, and BPh$_3$ at Room Temperature. A solution of allyl cyanide (3.1 μL, 38.5 μmol) and BPh$_3$ (9.4 mg, 38.8 μmol) in THF-d_8 was added to solid [(dippe)Ni(μ-H)]$_2$ (12.1 mg, 18.8 μmol). H$_2$ gas was immediately evolved, and the solution turned dark yellow-brown. A ^{31}P NMR spectrum taken after 20 min showed 66% **4** and 34% **5**. After the mixture was allowed to stand at room temperature for 18 h, was heated at 55 °C for 9 h, and was heated at 80 °C for 16 h, **5** had increased to 84% at the expense of **4**. **5/6** increased to 91% on addition of another ~5 mg of BPh$_3$; yet another ~5 mg of BPh$_3$ resulted in complete conversion to **6**. Recrystallization from THF/pentane at -30 °C yielded a yellow crystal of **6** for X-ray diffraction.

Experimental Details of X-ray Structural Determinations. Single crystals of **2**, **4**, **5**, **6**, and *cis*-**7** were mounted under Paratone-8277 on glass fibers and immediately placed in a cold nitrogen stream at -80 °C on the X-ray diffractometer. The X-ray intensity data were collected on a standard Siemens SMART CCD Area Detector System equipped with a normal focus molybdenum-target X-ray tube operated at 2.0 kW (50 kV, 40 mA). A total of 1321 frames of data (1.3 hemispheres) were collected using a narrow frame method with scan widths of 0.3° in ω and exposure times of 30 s/frame using a detector-to-crystal distance of 5.09 cm (maximum 2θ angle of 56.54°) for all of the crystals. The total data collection time was approximately 13 h. Frames were integrated with the Siemens SAINT program to 0.75 Å for all of the data sets. The unit cell parameters for all of the crystals were based upon the least-squares refinement of three-dimensional centroids of >5000 reflections.[43] Data were corrected for absorption using the program SADABS.[44] Space group assignments were made on the basis of systematic absences and intensity statistics by using the XPREP program (Siemens, SHELXTL 5.04). The structures were solved by using direct methods and refined by full-matrix least-squares on F^2.[45] For all of the structures, the non-hydrogen atoms were refined with anisotropic thermal parameters (except **6**, as noted below) and hydrogens were included in idealized positions giving data:parameter ratios greater than 10:1. There was nothing unusual about the solution or refinement of any of the structures, with the exception of **6**. The CN group in the anion was modeled as being disordered 50/50 (a slight

(42) Because (dippe)Ni(CN)$_2$ precipitates from solution, integration of the ^{31}P NMR resonance at 90.9 ppm does not measure the full extent of decomposition to this species. Addition of an internal standard (Ph$_3$P=O) to the reaction mixture, however, showed that $\leq$5% of the total amount of dippe present at the beginning of the reaction had disappeared from solution by the end, providing an upper limit of ~10% for the amount of (dippe)-Ni(CN)$_2$ formed in the reaction. Also, note that less decomposition was observed at low temperatures as compared to that observed at high temperatures.

(43) It has been noted that the integration program SAINT produces cell constant errors that are unreasonably small, because systematic error is not included. More reasonable errors might be estimated at 10× the listed value.
(44) The SADABS program is based on the method of Blessing, see: Blessing, R. H. *Acta Crystallogr., Sect. A* **1995**, *51*, 33–38.
(45) Using the SHELX95 package, $R_1 = (\sum ||F_o| - |F_c||)/\sum|F_o|$, w$R_2 = \{\sum[w(F_o^2 - F_c^2)^2]/\sum[w(F_o^2)^2]\}^{1/2}$, where $w = 1/[\sigma^2(F_o^2) + (a \cdot P)^2 + b \cdot P]$ and $P = [f \cdot (\text{maximum of 0 or } F_o^2) + (1 - f) \cdot F_c^2]$.

difference in thermal parameters was noted if a single orientation was chosen, see Supporting Information Figure S-13), using the Shelx SAME instruction to keep the two B−N−C geometries similar (see Supporting Information p S-48). The C and N atoms were kept isotropic in the refinement. Positional parameters for all atoms, anisotropic thermal parameters, all bond lengths and angles, as well as fixed hydrogen positional parameters are given in the Supporting Information for all of the structures.

Note Added in Proof. In addition to the NMR evidence for the orientation of the CN group in **5**, the X-ray structure of a single crystal obtained from a toluene solution of **5** is consistent with this assignment. The structure is isomorphic and isostructural with that of **4**. While it can be difficult to distinguish C and N atoms by X-ray diffraction, in this case refinement of the structure as the Ni−N−C−B isomer **5** clearly gives a better model for the bridging atoms than refinement as the Ni−C−N−B isomer **4** (see Supporting Information).

Supporting Information Available: Complete NMR data for **1**, **2**, **3**, **4**, **6**, and **7**; a diagram of the special apparatus for the preparation of **1** in an NMR tube; ^{1}H NMR spectra of *cis*-**2**, *trans*-**2**, *cis*-**7**, and *trans*-**7**; VT NMR data for **3**, **4**, **5**, and **6**; distribution of species plots (similar to Figure 1) showing experimental and calculated data for the C−H and C−CN activation of **1** (Scheme 1) at 20, 30, 35, 40, and 50 °C; X-ray crystallographic data for **2**, **4**, **5**, **6**, and *cis*-**7**, including tables of positional parameters for all atoms, anisotropic thermal parameters, all bond lengths and angles, and fixed hydrogen positional parameters (PDF and CIF). This material is available free of charge via the Internet at http://pubs.acs.org.

JA037002E